Meso-scale structures in bidisperse fluidized suspensions

William Holloway, Sofiane Benyahia, Christine Hrenya, and Sankaran Sundaresan

NETL Workshop on Multiphase Flow Science
Pittsburgh, PA, 2010

Outline

- Project objective
- Current status of GHD theory in MFIX
- Connection to Roadmap
- Model framework
- Test cases
- Model predictions
- Grid resolution effects
- Range of validity of kinetic theory formulation
- Summary

Project objective

Goal:

Study the segregation behavior of binary gas-solid flows in risers predicted by the kinetic theory model framework of Garzó, Hrenya, and Dufty[1] (GHD theory) with the fluid-particle drag model developed by Holloway, Yin and Sundaresan (HYS).[2,3,4]

[1] Garzó, Hrenya, and Dufty, *Phys. Rev. E*, 2007
[2] Holloway, Yin, and Sundaresan, *AIChE J.*, 2010
[3] Yin and Sundaresan, *AIChE J.*, 2009
[4] Yin and Sundaresan, *Ind. Eng. Chem. Res.*, 2008

Project objective

Goal:

Study the segregation behavior of binary gas-solid flows in risers predicted by the kinetic theory model framework of Garzó, Hrenya, and Dufty[1] (GHD theory) with the fluid-particle drag model developed by Holloway, Yin and Sundaresan (HYS).[2,3,4]

Necessitates the robust operation of HYS drag model and GHD theory in MFIX.

[1] Garzó, Hrenya, and Dufty, *Phys. Rev. E*, 2007
[2] Holloway, Yin, and Sundaresan, *AIChE J.*, 2010
[3] Yin and Sundaresan, *AIChE J.*, 2009
[4] Yin and Sundaresan, *Ind. Eng. Chem. Res.*, 2008

Project objective

Goal:

Study the segregation behavior of binary gas-solid flows in risers predicted by the kinetic theory model framework of Garzó, Hrenya, and Dufty[1] (GHD theory) with the fluid-particle drag model developed by Holloway, Yin and Sundaresan (HYS).[2,3,4]

Demonstrated

Necessitates the robust operation of HYS drag model and GHD theory in MFIX.

[1]Garzó, Hrenya, and Dufty, *Phys. Rev. E*, 2007
[2]Holloway, Yin, and Sundaresan, *AIChE J.*, 2010
[3]Yin and Sundaresan, *AIChE J.*, 2009
[4]Yin and Sundaresan, *Ind. Eng. Chem. Res.*, 2008

Project objective

Goal:

Study the segregation behavior of binary gas-solid flows in risers predicted by the kinetic theory model framework of Garzó, Hrenya, and Dufty[1] (GHD theory) with the fluid-particle drag model developed by Holloway, Yin and Sundaresan (HYS).[2,3,4]

Demonstrated

Necessitates the robust operation of HYS drag model and GHD theory in MFIX.

Current focus

[1]Garzó, Hrenya, and Dufty, *Phys. Rev. E*, 2007
[2]Holloway, Yin, and Sundaresan, *AIChE J.*, 2010
[3]Yin and Sundaresan, *AIChE J.*, 2009
[4]Yin and Sundaresan, *Ind. Eng. Chem. Res.*, 2008

Current status of GHD theory in MFIX

Current status of GHD theory in MFIX

- GHD theory has been successfully incorporated within the MFIX framework and has been tested extensively.

Current status of GHD theory in MFIX

- GHD theory has been successfully incorporated within the MFIX framework and has been tested extensively.
- The GHD theory implementation has operated robustly for both homogeneous and inhomogeneous gas-solid flows with binary particle size distributions (PSD).

Current status of GHD theory in MFIX

- GHD theory has been successfully incorporated within the MFIX framework and has been tested extensively.
- The GHD theory implementation has operated robustly for both homogeneous and inhomogeneous gas-solid flows with binary particle size distributions (PSD).
- Currently GHD theory implementation is only compatible with binary mixtures.

Current status of GHD theory in MFIX

- GHD theory has been successfully incorporated within the MFIX framework and has been tested extensively.
- The GHD theory implementation has operated robustly for both homogeneous and inhomogeneous gas-solid flows with binary particle size distributions (PSD).
- Currently GHD theory implementation is only compatible with binary mixtures.
- Only two drag relations have been implemented with GHD theory at this point (namely, HYS and Wen-Yu).

Connection to Roadmap

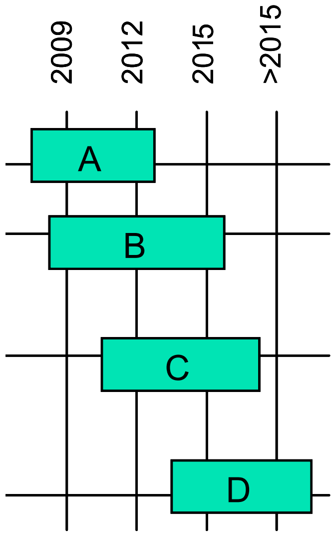

Connection to Roadmap

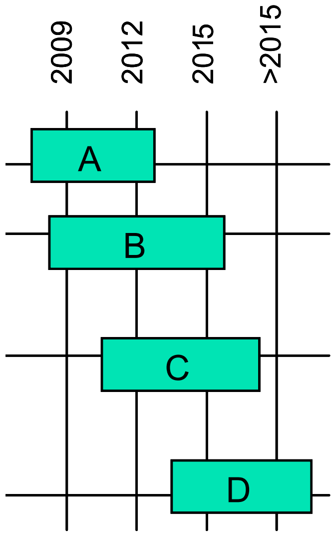

Princeton Tasks

Task 4.6:

The MFIX framework, modified to account for the new physical models will be developed as part of this work and compared to experimental data obtained from high-velocity systems.

Connection to Roadmap

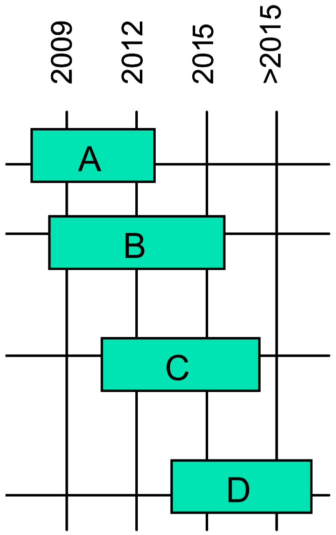

Princeton Tasks

Roadmap

Task 4.6:

The MFIX framework, modified to account for the new physical models will be developed as part of this work and compared to experimental data obtained from high-velocity systems.

Near Term:

- Perform high-fidelity, transient 3-D multiphase flow computations with PSD (particle size distribution).
- Identify deficiencies of current models developed for gas-solid flows.

Continuum models for polydisperse flows

[1]Garzó, Hrenya, and Dufty, *Phys. Rev. E*, 2007

Continuum models for polydisperse flows

Continuity

$$\frac{\partial n_i}{\partial t} + \nabla \cdot (n_i \mathbf{V}) = -\frac{1}{m_i} \nabla \cdot \mathbf{j_{0_i}}$$

[1]Garzó, Hrenya, and Dufty, *Phys. Rev. E*, 2007

Continuum models for polydisperse flows

Continuity

$$\frac{\partial n_i}{\partial t} + \nabla \cdot (n_i \mathbf{V}) = -\frac{1}{m_i} \nabla \cdot \mathbf{j_{0_i}}$$

Momentum

$$\rho_s \phi \left(\frac{\partial \mathbf{V}}{\partial t} + \mathbf{V} \cdot \nabla \mathbf{V} \right) = -\nabla \cdot \sigma_{\mathbf{s}} + \sum_{i=1}^{s} n_i \mathbf{F_i}$$

$$\mathbf{j_{0_i}} = -\sum_{j=1}^{s} \frac{m_i m_j n_j}{\rho} D_{ij} \nabla ln(n_j) - \rho D_i^T \nabla ln(T) - \sum_{j=1}^{s} D_{ij}^F \mathbf{F_j}$$

[1]Garzó, Hrenya, and Dufty, *Phys. Rev. E*, 2007

Continuum models for polydisperse flows

Continuity

$$\frac{\partial n_i}{\partial t} + \nabla \cdot (n_i \mathbf{V}) = -\frac{1}{m_i} \nabla \cdot \mathbf{j_{0_i}}$$

Momentum

$$\rho_s \phi \left(\frac{\partial \mathbf{V}}{\partial t} + \mathbf{V} \cdot \nabla \mathbf{V} \right) = -\nabla \cdot \sigma_\mathbf{s} + \sum_{i=1}^{s} n_i \mathbf{F_i}$$

$$\mathbf{j_{0_i}} = -\sum_{j=1}^{s} \frac{m_i m_j n_j}{\rho} D_{ij} \nabla ln(n_j) - \rho D_i^T \nabla ln(T) - \sum_{j=1}^{s} D_{ij}^F \mathbf{F_j}$$

Fluctuating energy

$$\frac{3n}{2} \left(\frac{\partial T}{\partial t} + \mathbf{V} \cdot \nabla T \right) = -\nabla \cdot \mathbf{q} - \sigma_\mathbf{s} : \nabla \mathbf{V} - \frac{3n\zeta T}{2} + \frac{3T}{2} \sum_{i=1}^{s} \frac{1}{m_i} \nabla \cdot \mathbf{j_{0_i}} + \sum_{i=1}^{s} \frac{\mathbf{F_i} \cdot \mathbf{j_{0_i}}}{m_i}$$

$$\mathbf{q} = -\lambda \nabla T - \left(\sum_{i=1}^{s} \sum_{j=1}^{s} T^2 D_{q,ij} \nabla ln(n_j) + L_{ij} \mathbf{F_j} \right)$$

[1]Garzó, Hrenya, and Dufty, *Phys. Rev. E*, 2007

External forces in polydisperse systems

$$\mathbf{j_{0_i}} = -\sum_{j=1}^{s} \frac{m_i m_j n_j}{\rho} D_{ij} \nabla ln(n_j) - \rho D_i^T \nabla ln(T) - \sum_{j=1}^{s} D_{ij}^F \mathbf{F_j}$$

External forces in polydisperse systems

$$\mathbf{j_{0_i}} = -\sum_{j=1}^{s} \frac{m_i m_j n_j}{\rho} D_{ij} \nabla ln(n_j) - \rho D_i^T \nabla ln(T) - \sum_{j=1}^{s} D_{ij}^F \mathbf{F_j}$$

$$\mathbf{F_j} = m_j \mathbf{g} + V_j \nabla P_g + \mathbf{F_{Dj}}$$

External forces in polydisperse systems

$$\mathbf{j_{0_i}} = -\sum_{j=1}^{s} \frac{m_i m_j n_j}{\rho} D_{ij} \nabla ln(n_j) - \rho D_i^T \nabla ln(T) - \sum_{j=1}^{s} D_{ij}^F \mathbf{F_j}$$

$$\mathbf{F_j} = m_j \mathbf{g} + V_j \nabla P_g + \mathbf{F_{Dj}}$$

Fluid-particle drag model (HYS):[2,3,4]

$$\mathbf{F_{Dj}} = -\frac{\beta_j}{n_j} \left(\mathbf{V_j} - \mathbf{V_g}\right)$$

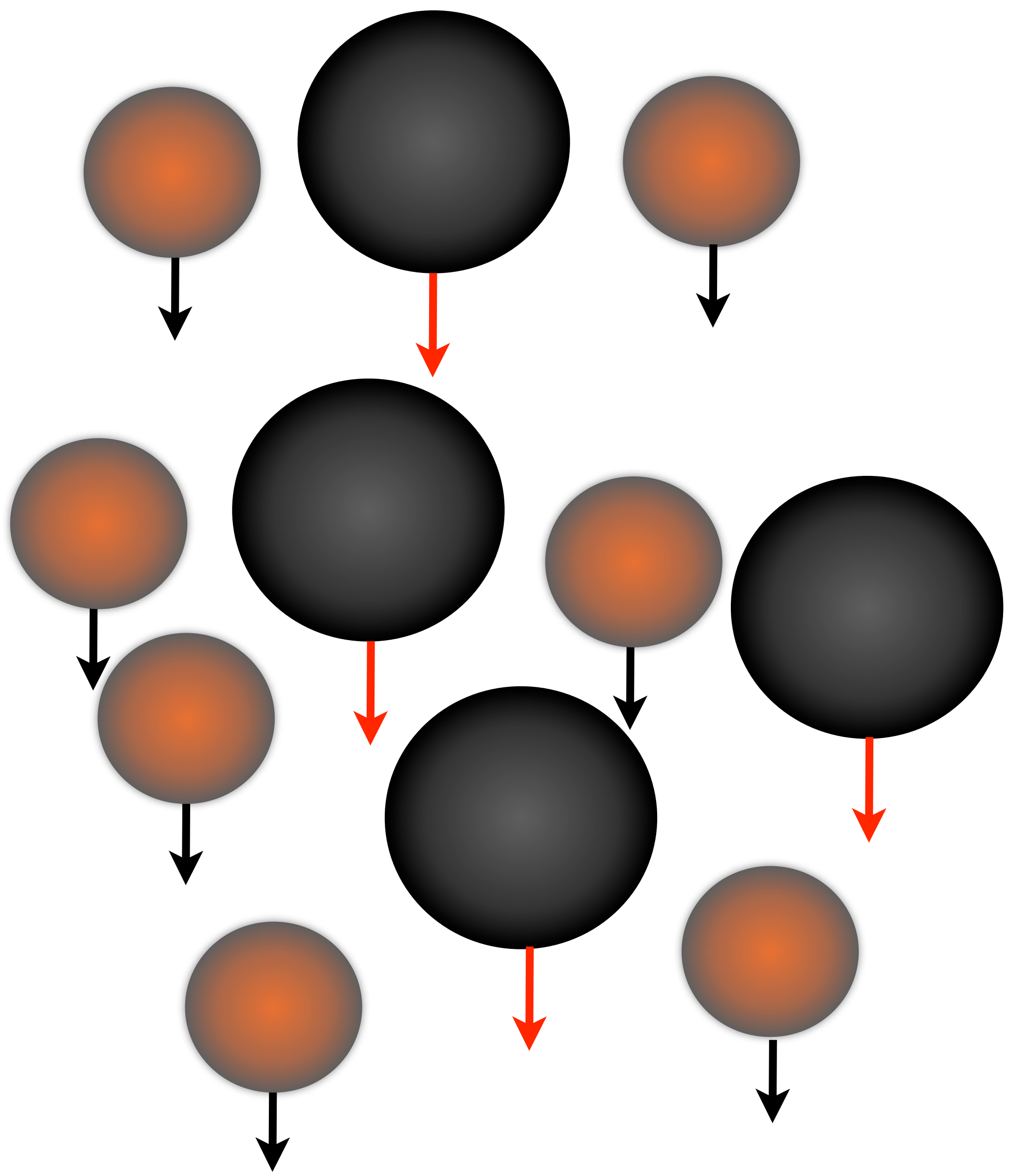

[2]Holloway, Yin, and Sundaresan, *AIChE J.*, 2010
[3]Yin and Sundaresan, *AIChE J.*, 2009
[4]Yin and Sundaresan, *Ind. Eng. Chem. Res.*, 2008

External forces in polydisperse systems

$$\mathbf{j_{0_i}} = -\sum_{j=1}^{s} \frac{m_i m_j n_j}{\rho} D_{ij} \nabla ln(n_j) - \rho D_i^T \nabla ln(T) - \sum_{j=1}^{s} D_{ij}^F \mathbf{F_j}$$

$$\mathbf{F_j} = m_j \mathbf{g} + V_j \nabla P_g + \mathbf{F_{Dj}}$$

Fluid-particle drag model (HYS):[2,3,4]

$$\mathbf{F_{Dj}} = -\frac{\beta_j}{n_j}(\mathbf{V_j} - \mathbf{V_g}) - \sum_{i \neq j}^{s} \frac{\beta_{ji}}{n_j}(\mathbf{V_i} - \mathbf{V_j})$$

$$\beta_{ji} = -\frac{2\alpha\phi_i\phi_j}{\frac{\phi_i}{\beta_i} + \frac{\phi_j}{\beta_j}}$$

Off-diagonal friction coefficient

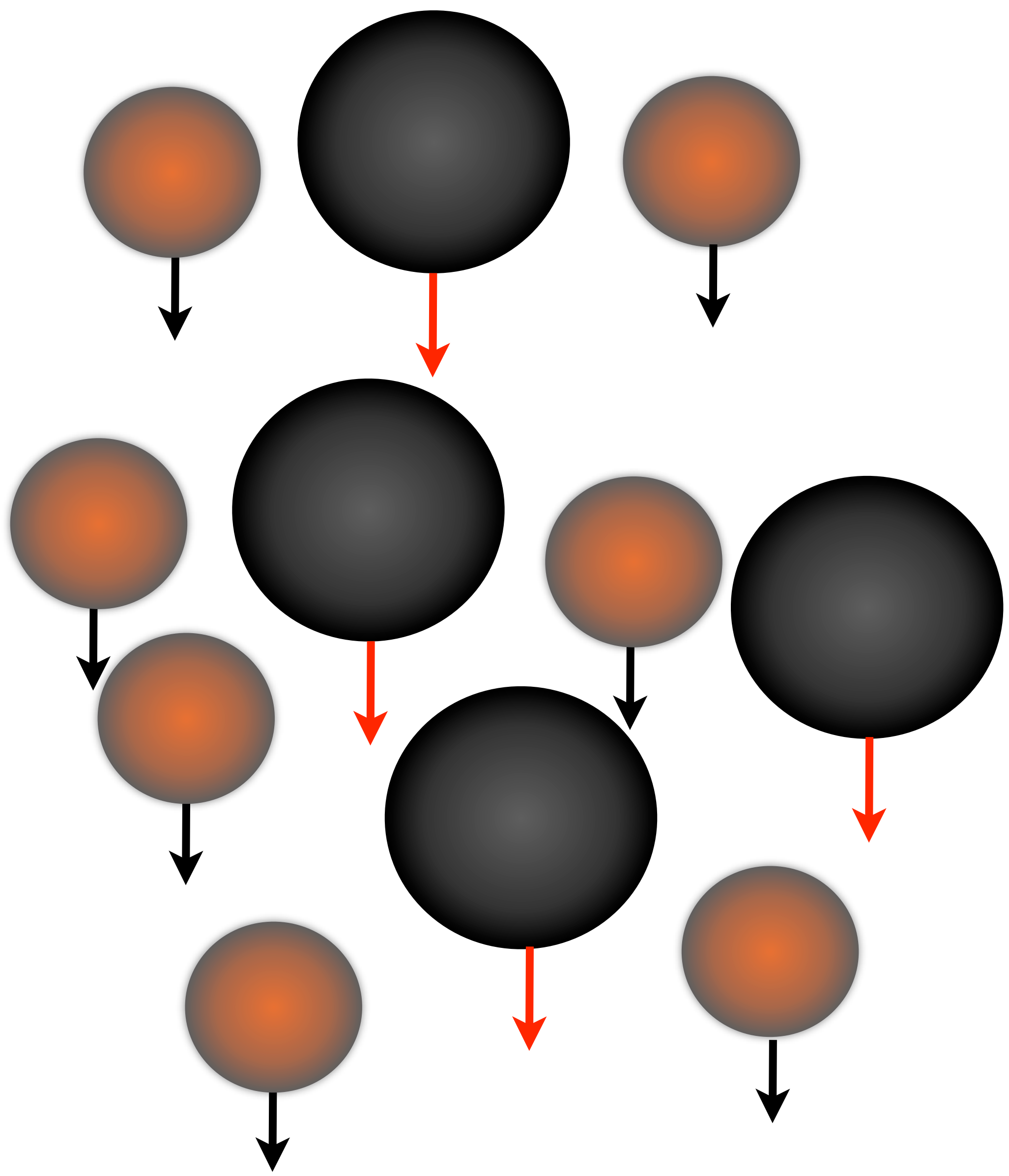

[2]Holloway, Yin, and Sundaresan, *AIChE J.*, 2010
[3]Yin and Sundaresan, *AIChE J.*, 2009
[4]Yin and Sundaresan, *Ind. Eng. Chem. Res.*, 2008

Test cases

Broad PSD

Test cases

Broad PSD

- Binary approximation
  - $d_1 = 212.5\ \mu m$, $d_2 = 127.5\ \mu m$
  - $\phi = 0.15$

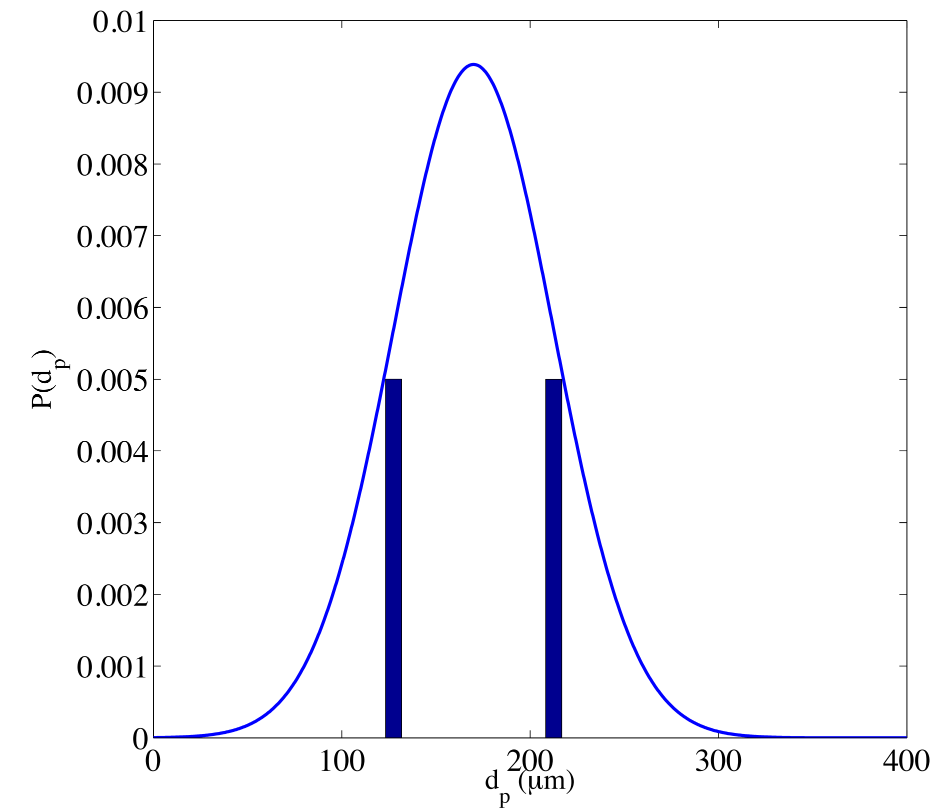

Test cases

Broad PSD

- Binary approximation
  - $d_1 = 212.5\ \mu\text{m}$, $d_2 = 127.5\ \mu\text{m}$
  - $\phi = 0.15$
- Monodisperse approximation
  - $d = 170\ \mu\text{m}$
  - $\phi = 0.15$

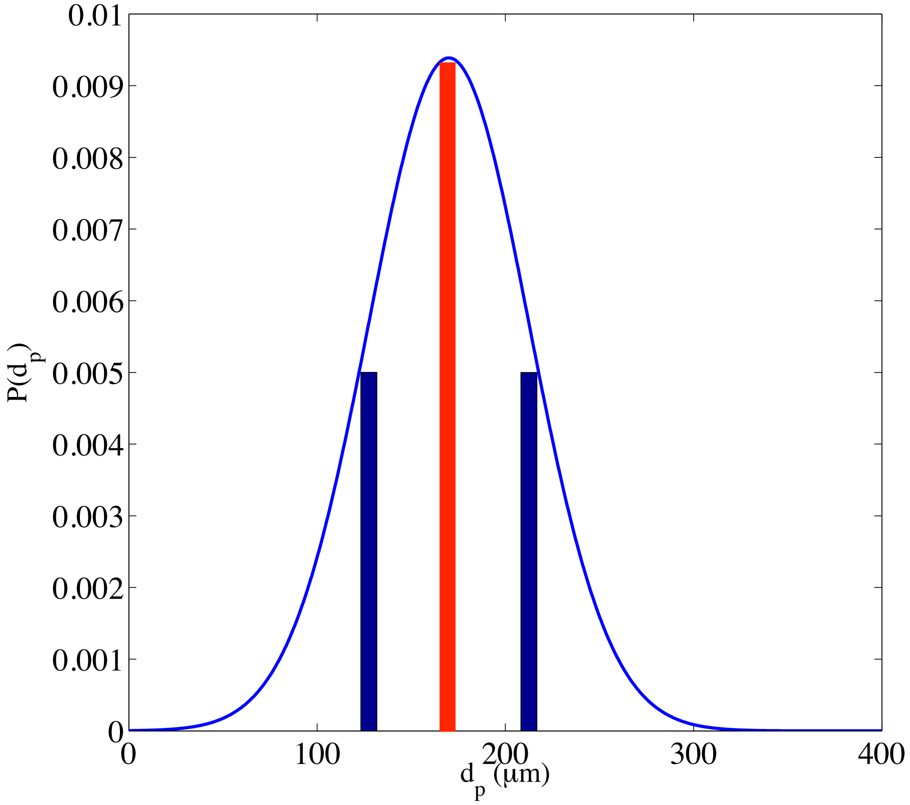

Test cases

Broad PSD

- Binary approximation
  - $d_1 = 212.5\ \mu\text{m}, d_2 = 127.5\ \mu\text{m}$
  - $\phi = 0.15$
- Monodisperse approximation
  - $d = 170\ \mu\text{m}$
  - $\phi = 0.15$

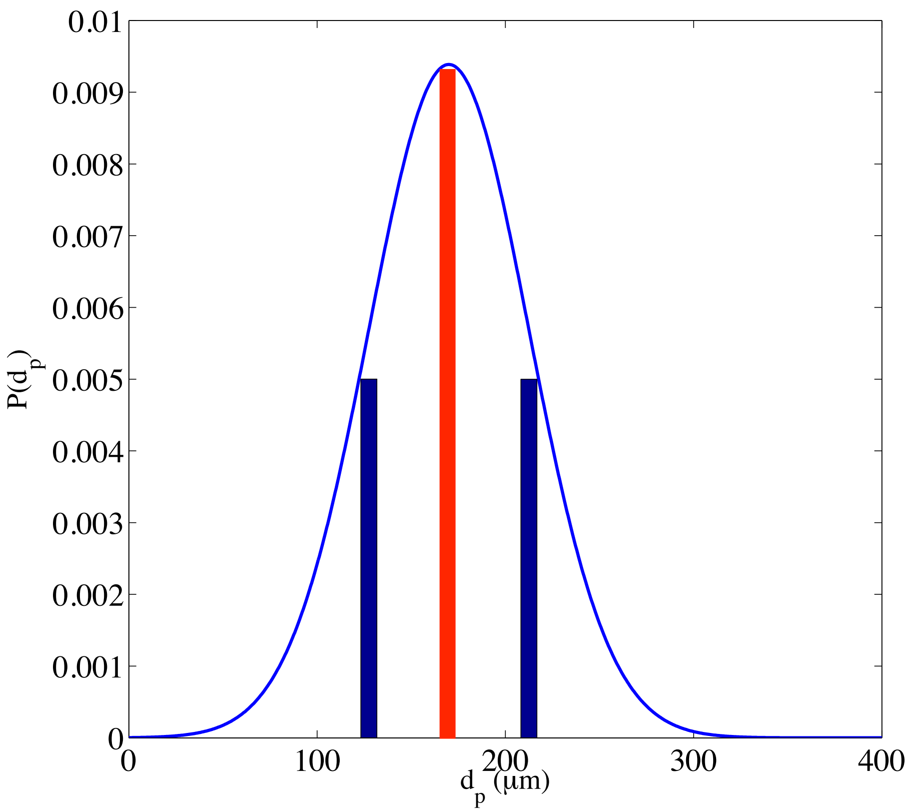

Bimodal PSD with disparate size ratio

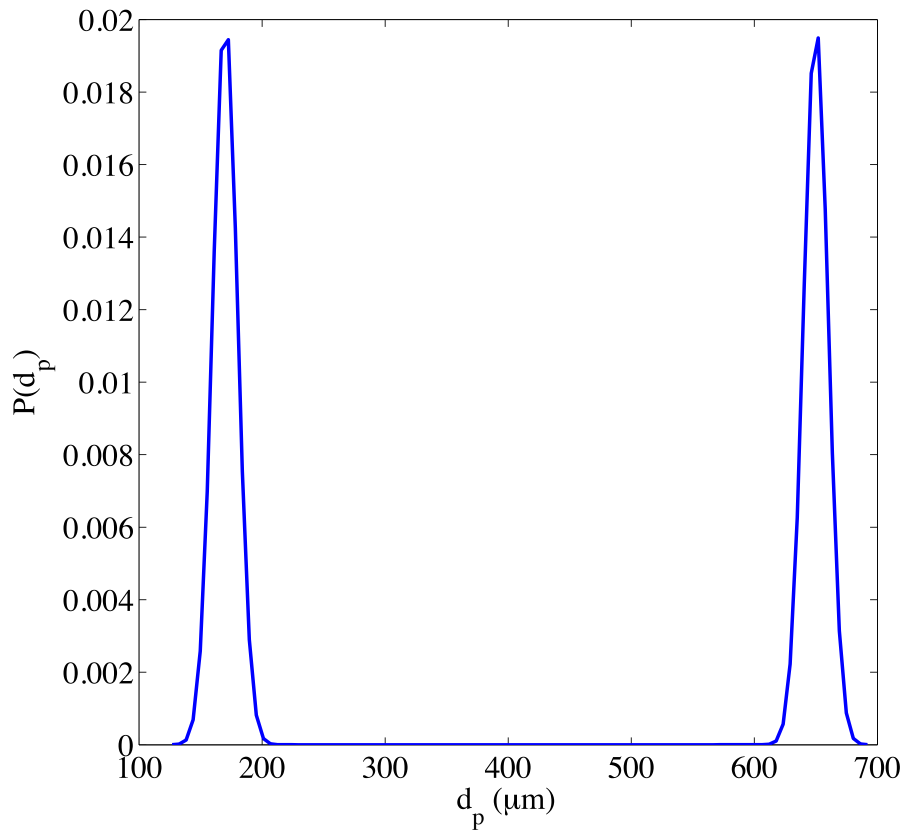

Test cases

Broad PSD

- Binary approximation
  - $d_1 = 212.5\ \mu m, d_2 = 127.5\ \mu m$
  - $\phi = 0.15$
- Monodisperse approximation
  - $d = 170\ \mu m$
  - $\phi = 0.15$

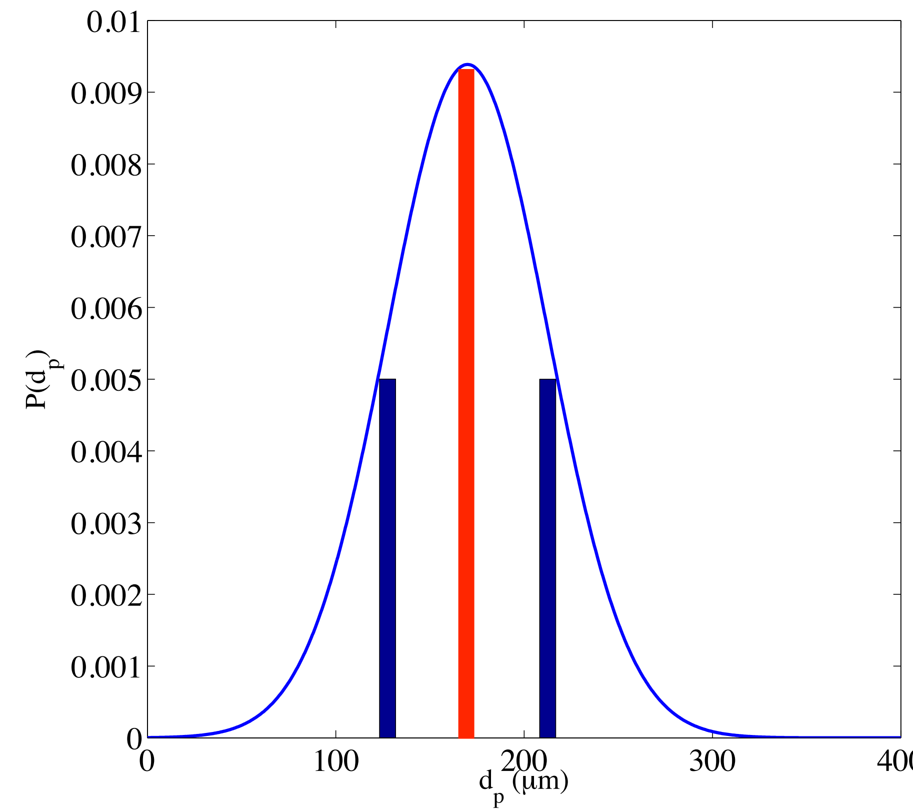

Bimodal PSD with disparate size ratio

- Binary approximation
  - $d_1 = 650\ \mu m, d_2 = 170\ \mu m$
  - $\phi = 0.15$

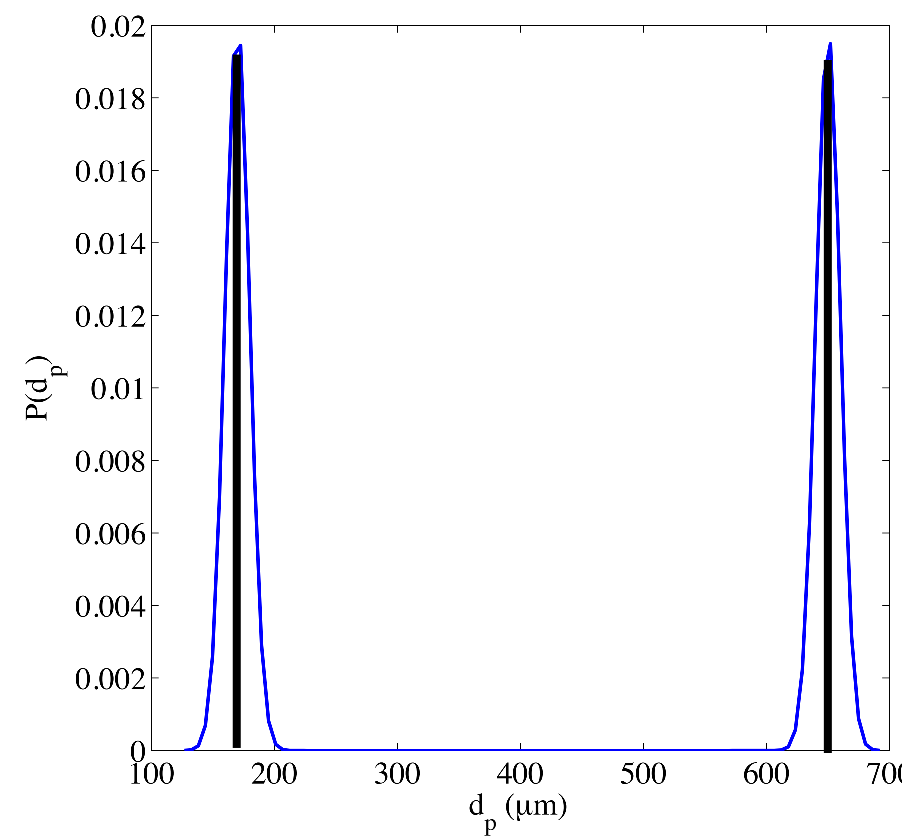

Test cases

Broad PSD

- Binary approximation
  - $d_1 = 212.5\ \mu m, d_2 = 127.5\ \mu m$
  - $\phi = 0.15$
- Monodisperse approximation
  - $d = 170\ \mu m$
  - $\phi = 0.15$

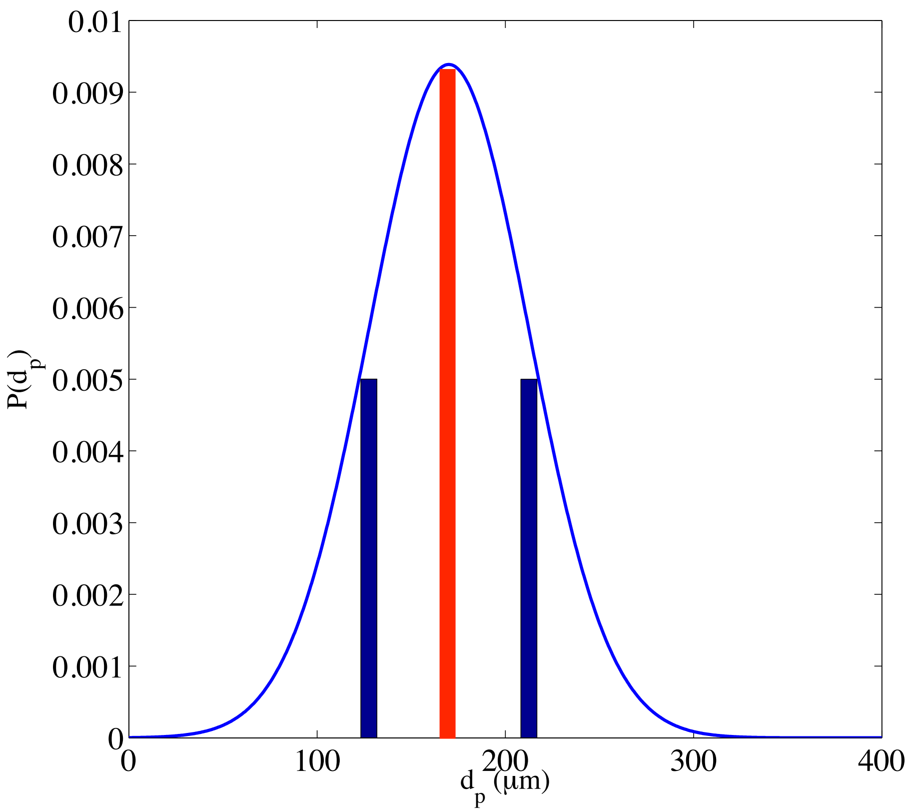

Bimodal PSD with disparate size ratio

- Binary approximation
  - $d_1 = 650\ \mu m, d_2 = 170\ \mu m$
  - $\phi = 0.15$
- Monodisperse approximation
  - $d = 270\ \mu m$
  - $\phi = 0.15$

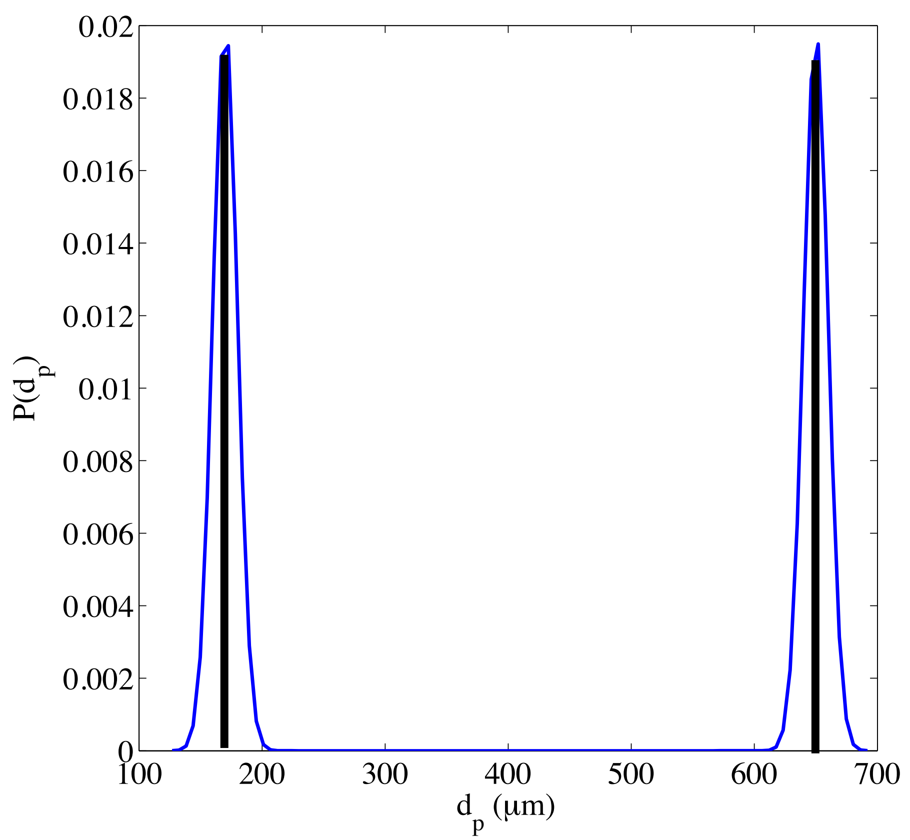

Model predictions

Broad PSD ($e = 0.95$)

Model predictions

Broad PSD (e = 0.95)

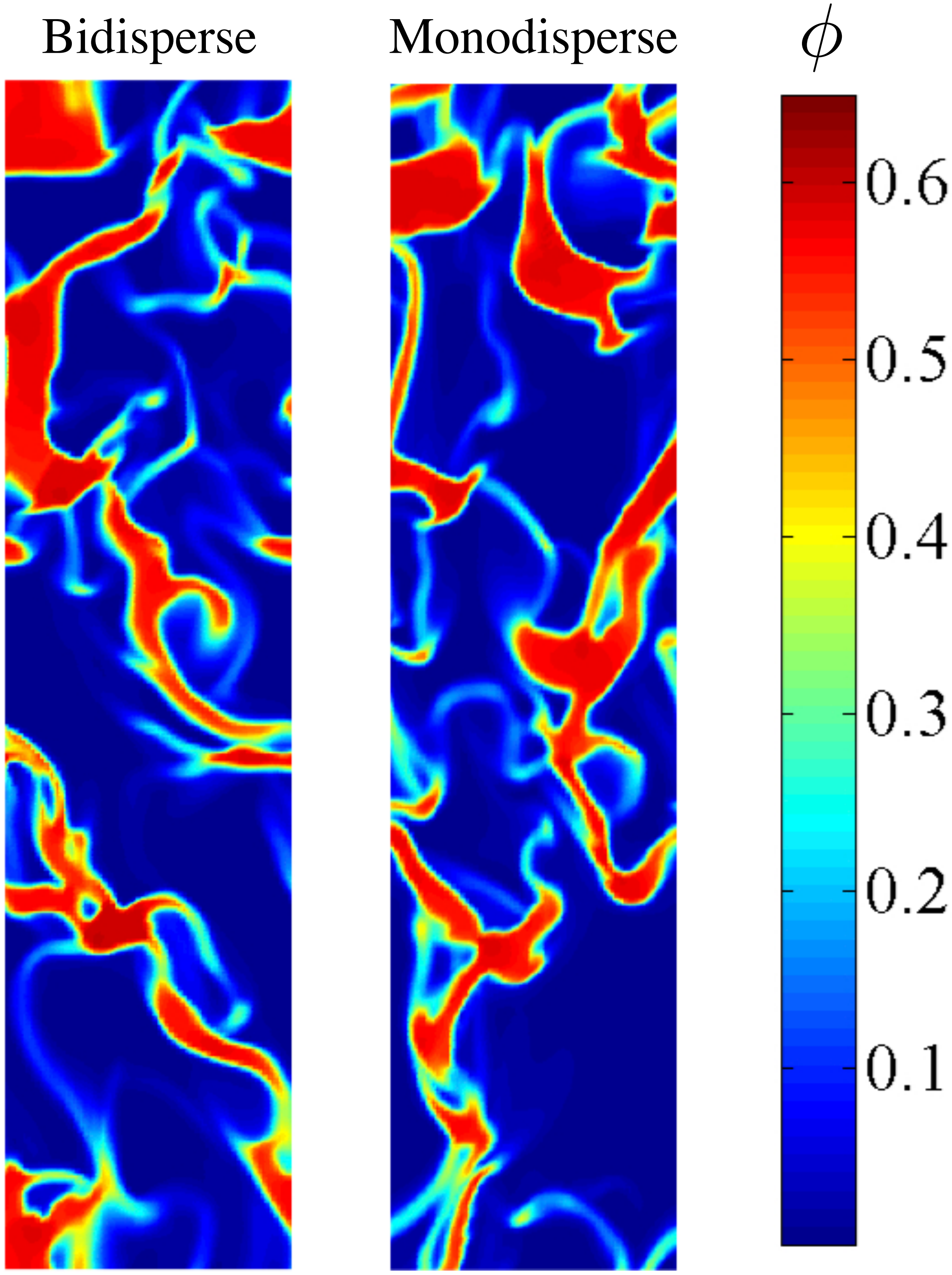

MFIX simulations:

- d_1=212.5 μm, d_2=127.5 μm
- $\langle\phi_1\rangle$= 0.125, $\langle\phi_2\rangle$= 0.025
- Doubly periodic
- 16 cm x 64 cm
- 0.25 cm grids

Model predictions

Broad PSD ($e = 0.95$)

Bidisperse Monodisperse ϕ

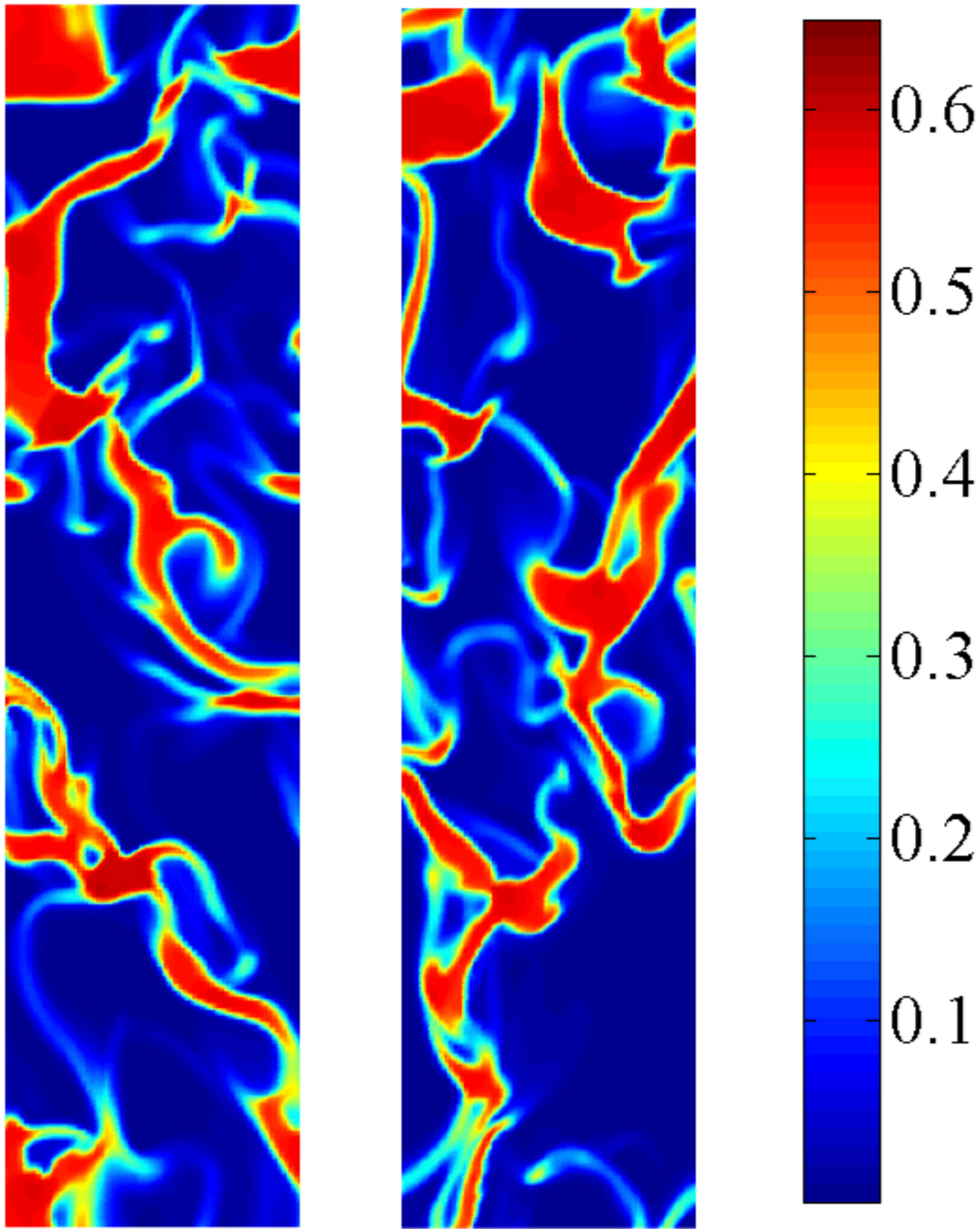

$$\langle V_{slip} \rangle = \frac{\langle (1-\phi) V_g \rangle}{\langle 1-\phi \rangle} - \frac{\langle \phi V_{s_{mix}} \rangle}{\langle \phi \rangle}$$

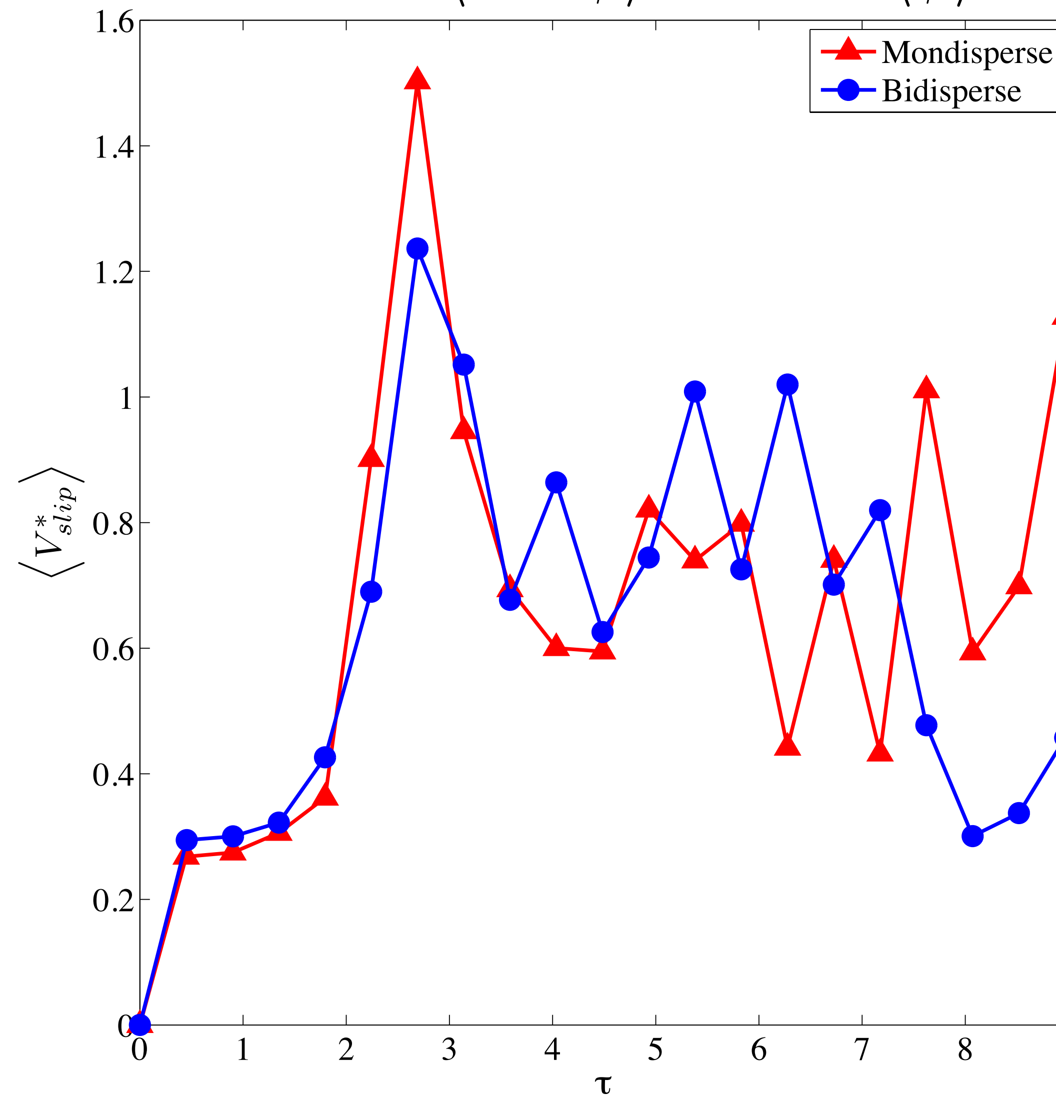

$$\langle V^*_{slip} \rangle = \frac{\langle V_{slip} \rangle}{V_t}$$

$$\tau = t \frac{g}{V_t}$$

MFIX simulations:

- d_1=212.5 μm, d_2=127.5 μm
- $\langle \phi_1 \rangle$= 0.125, $\langle \phi_2 \rangle$= 0.025
- Doubly periodic
- 16 cm x 64 cm
- 0.25 cm grids

Model predictions

Broad PSD ($e = 0.99$)

Model predictions

Broad PSD (e = 0.99)

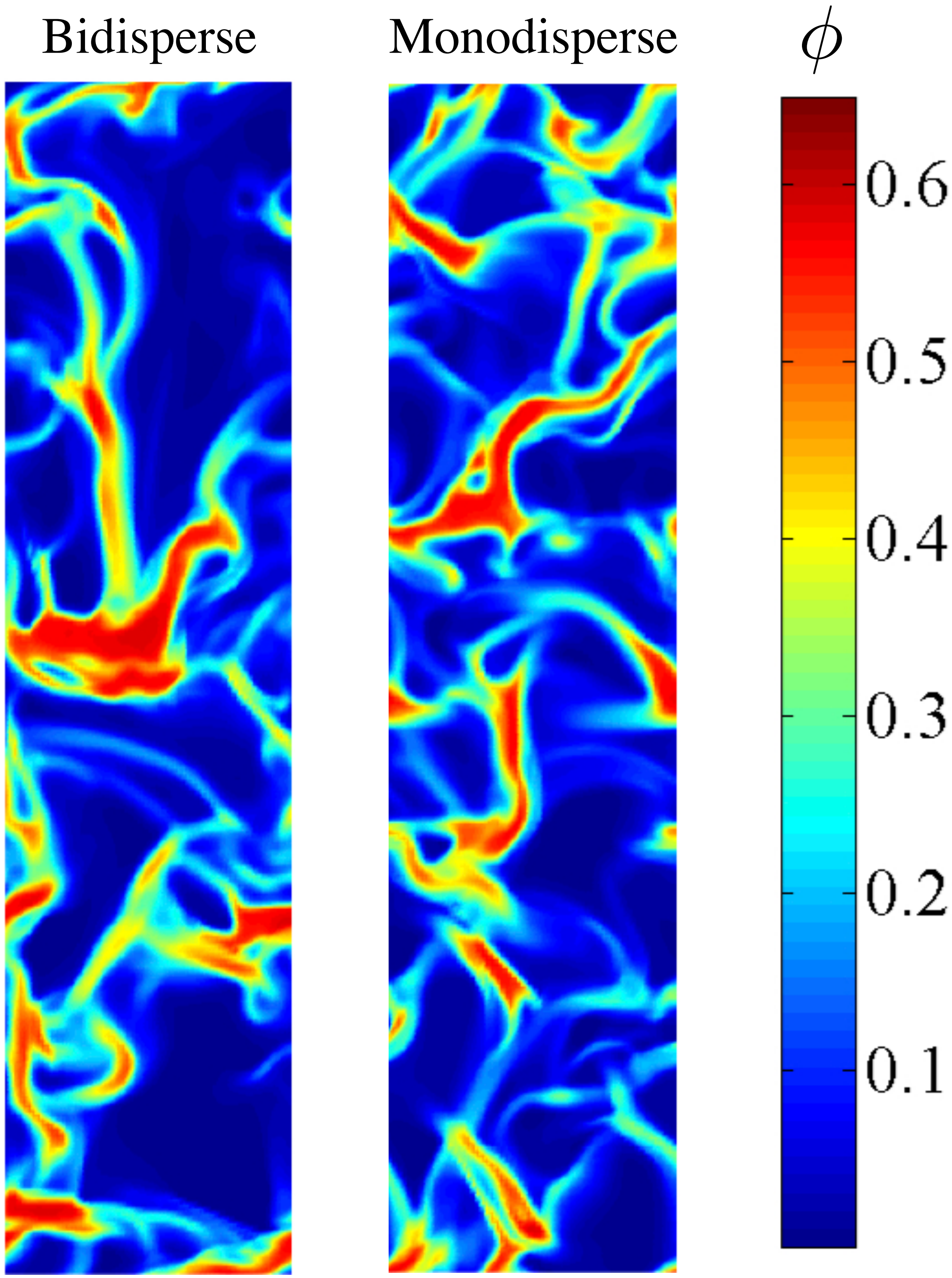

MFIX simulations:

- d_1=212.5 μm, d_2=127.5 μm
- $\langle\phi_1\rangle$= 0.125, $\langle\phi_2\rangle$= 0.025
- Doubly periodic
- 16 cm x 64 cm
- 0.25 cm grids

Model predictions

Broad PSD ($e = 0.99$)

Bidisperse Monodisperse ϕ

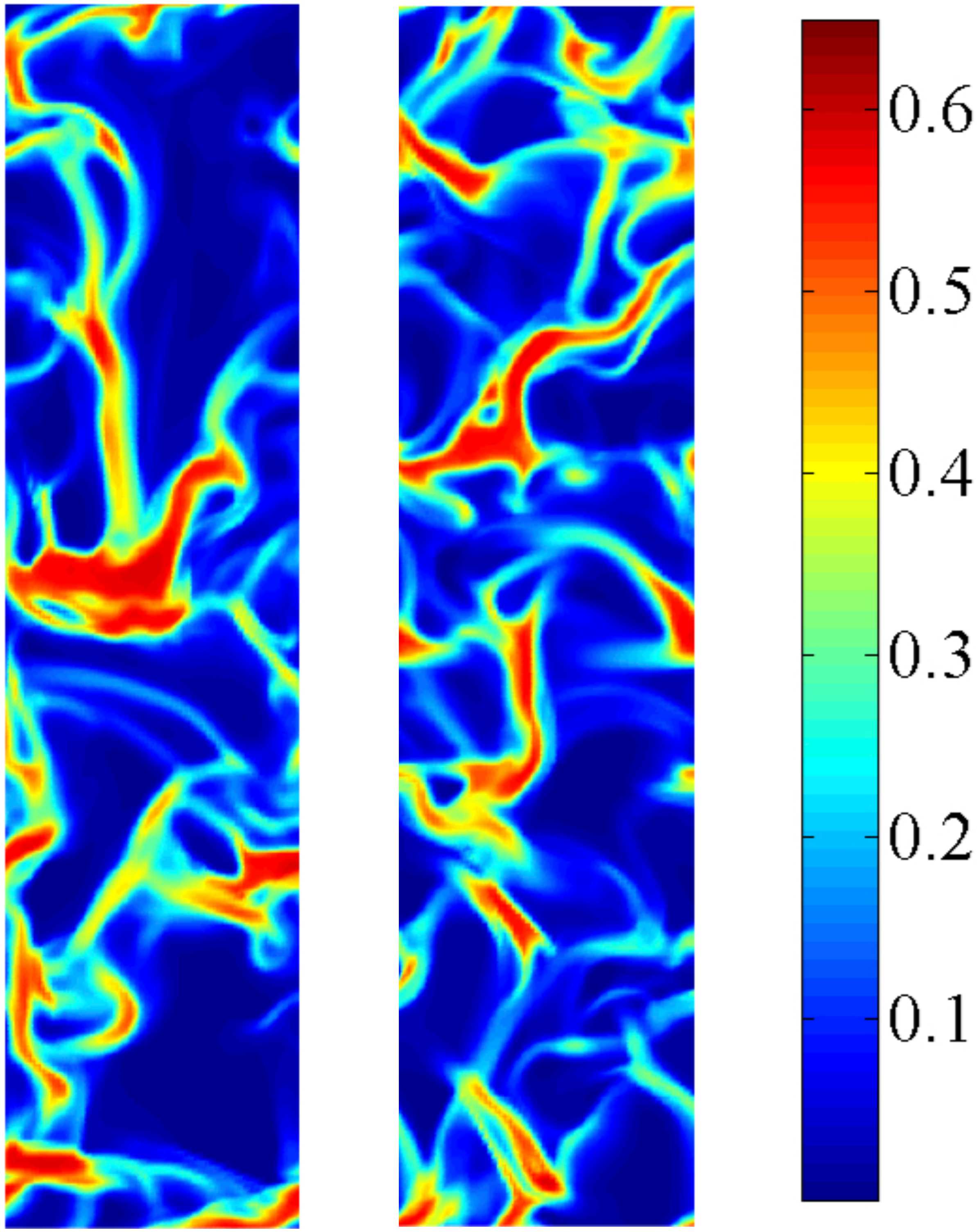

$$\langle V_{slip} \rangle = \frac{\langle (1-\phi) V_g \rangle}{\langle 1-\phi \rangle} - \frac{\langle \phi V_{s_{mix}} \rangle}{\langle \phi \rangle}$$

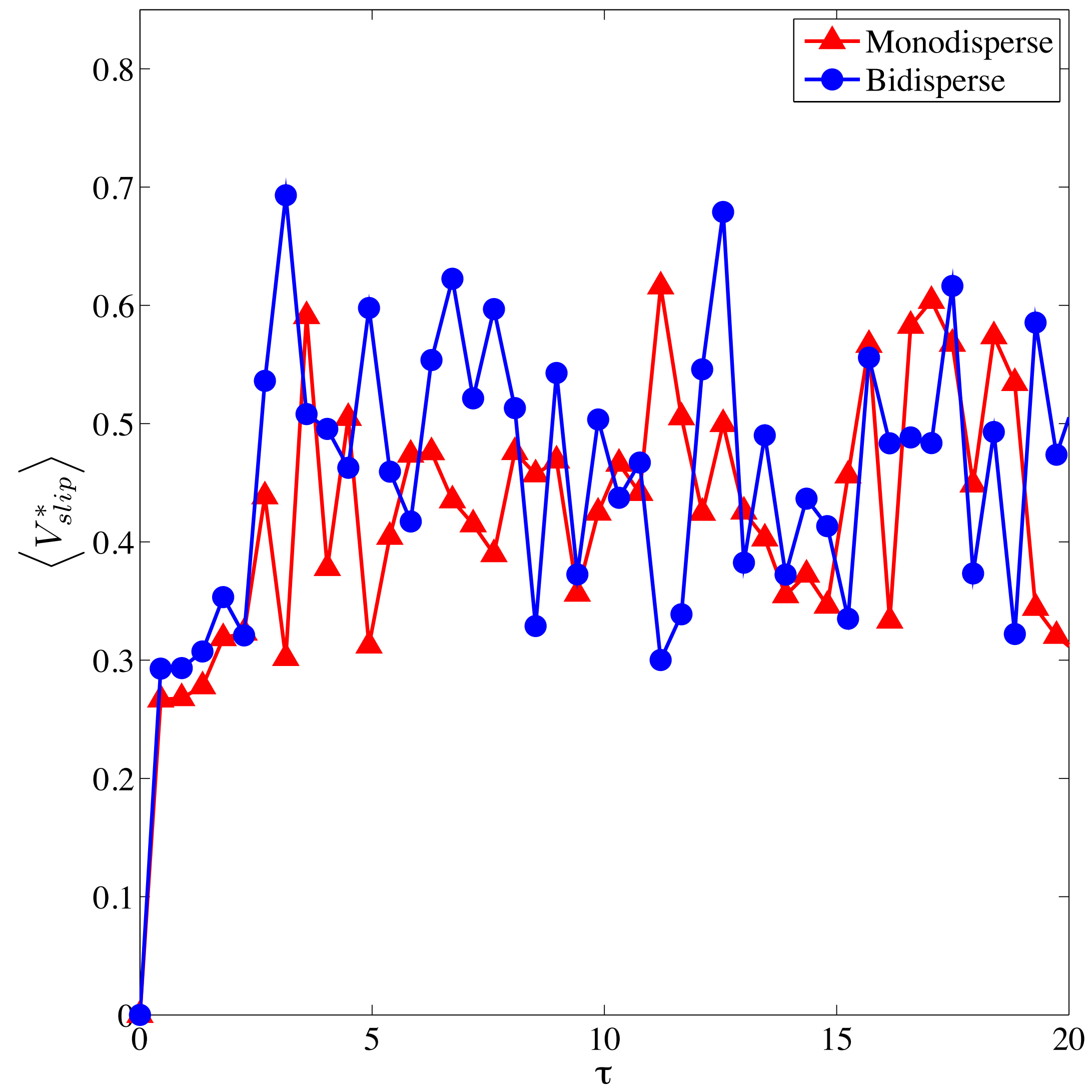

MFIX simulations:

- d_1=212.5 μm, d_2=127.5 μm
- $\langle \phi_1 \rangle$= 0.125, $\langle \phi_2 \rangle$= 0.025
- Doubly periodic
- 16 cm x 64 cm
- 0.25 cm grids

$$\langle V^*_{slip} \rangle = \frac{\langle V_{slip} \rangle}{V_t}$$

$$\tau = t \frac{g}{V_t}$$

Model prediction: Volume fraction ratios

Broad PSD

Model prediction: Volume fraction ratios

Broad PSD

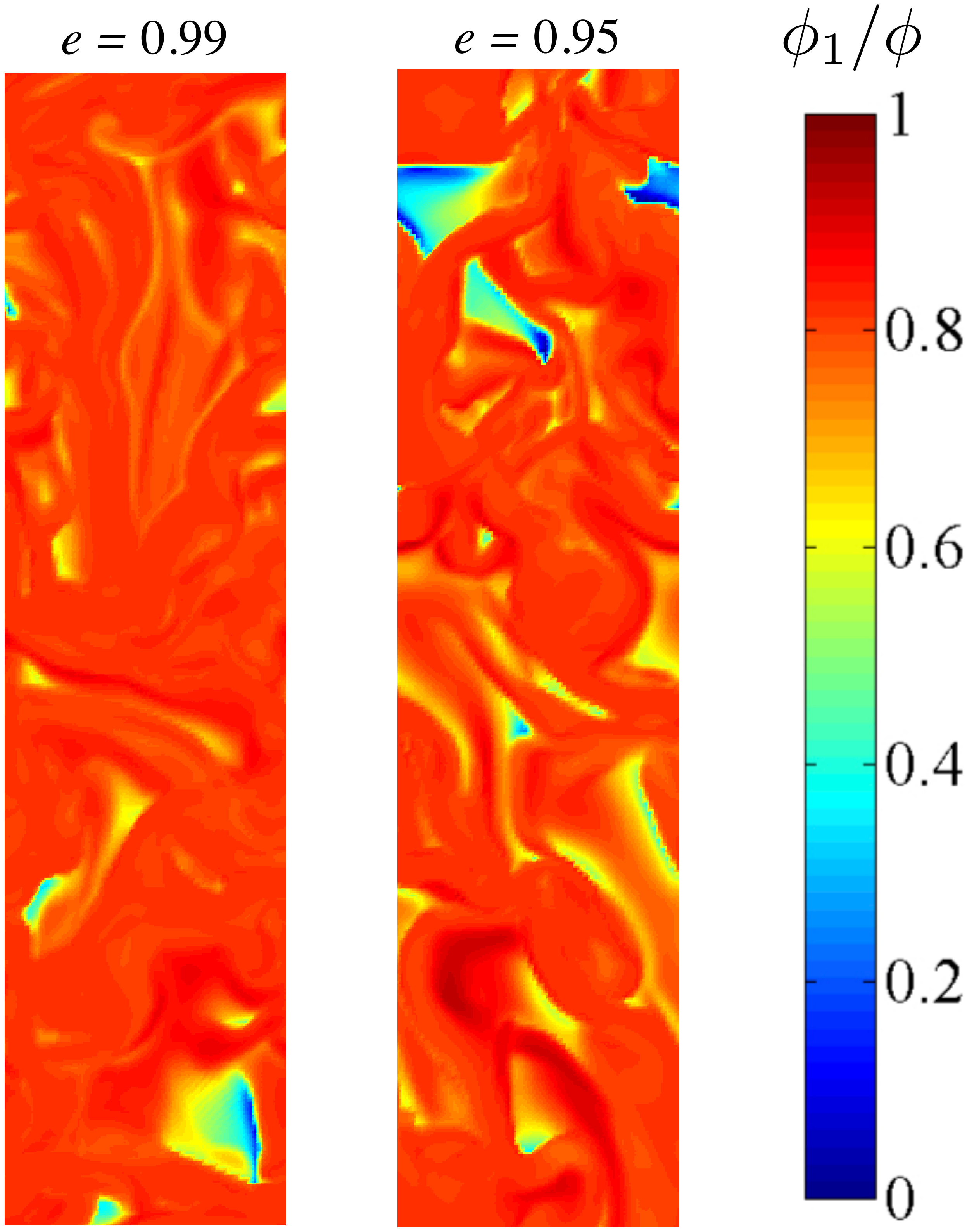

MFIX simulations:

- GHD theory
- HYS drag model
- d_1=212.5 μm, d_2=127.5 μm
- $\langle\phi_1\rangle$= 0.125, $\langle\phi_2\rangle$= 0.025
- Doubly periodic
- 16 cm x 64 cm

Model prediction: Volume fraction ratios

Broad PSD

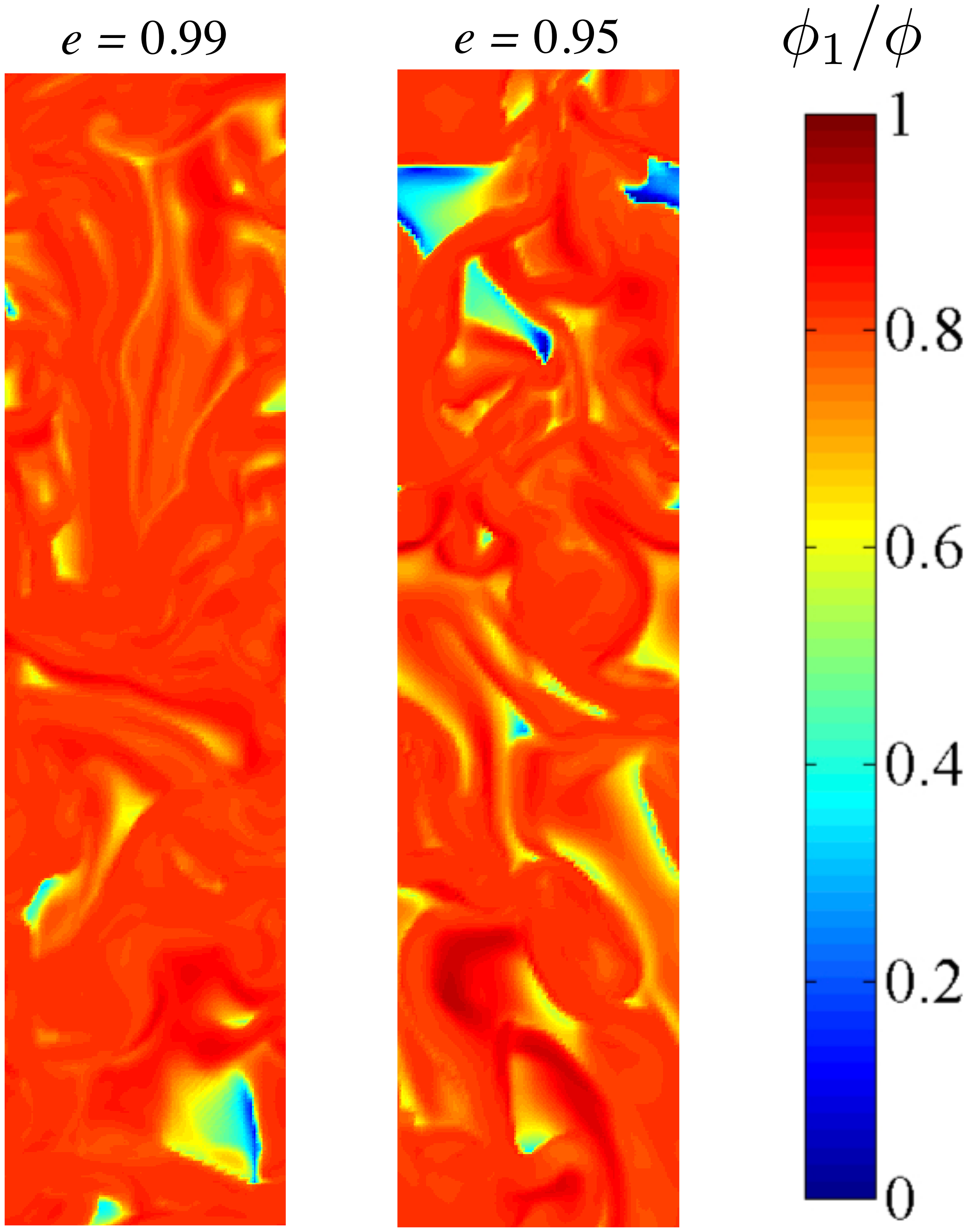

MFIX simulations:

- GHD theory
- HYS drag model
- d_1=212.5 μm, d_2=127.5 μm
- $\langle\phi_1\rangle$= 0.125, $\langle\phi_2\rangle$= 0.025
- Doubly periodic
- 16 cm x 64 cm

Broad PSD maintains a very tight distribution of volume fraction ratio throughout the flow domain for both coefficients of restitution.

Model predictions

Bimodal PSD ($e = 0.95$)

Model predictions

Bimodal PSD ($e = 0.95$)

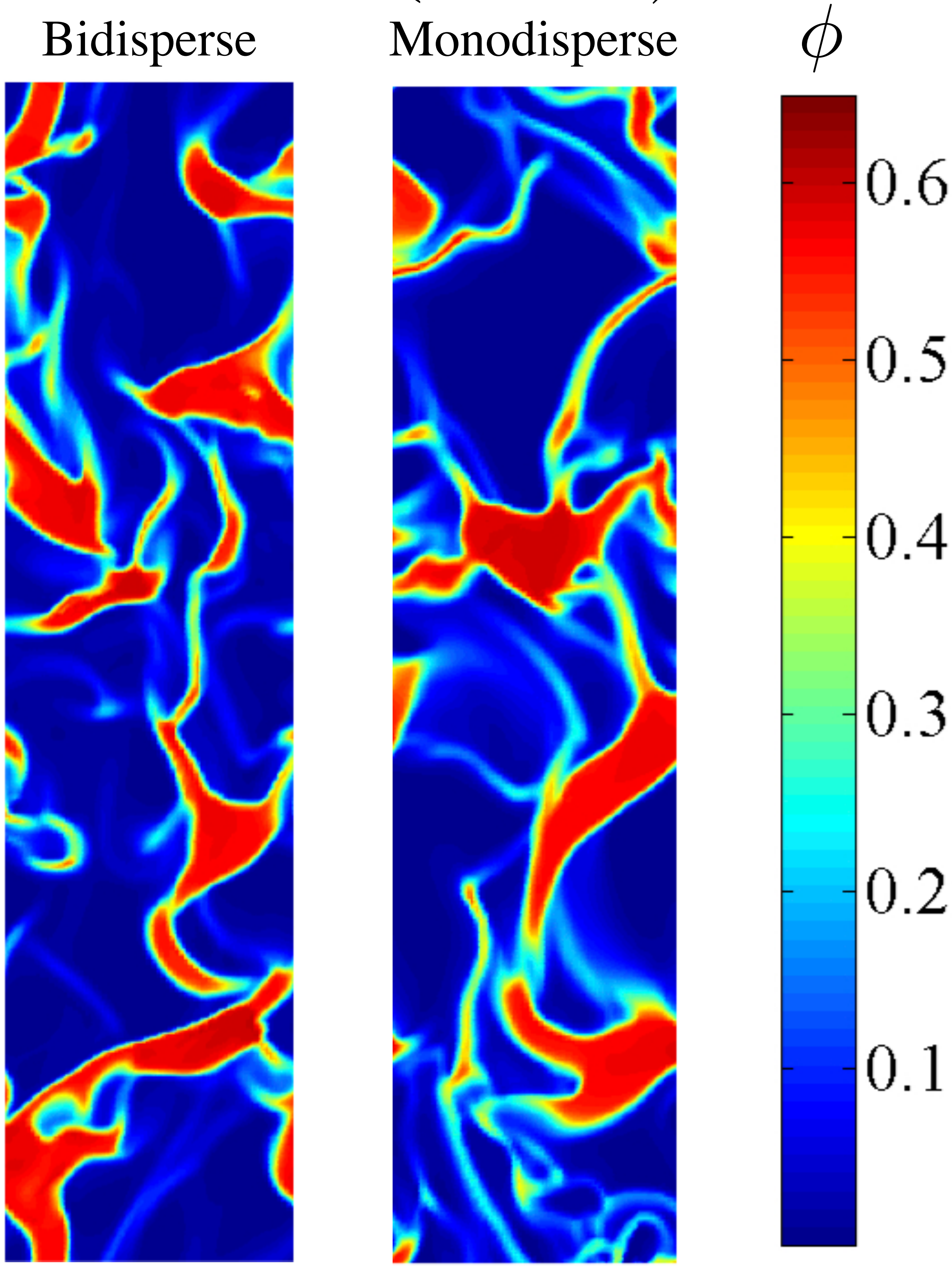

MFIX simulations:

- d_1=650 μm, d_2=170 μm
- $\langle \phi_1 \rangle = \langle \phi_2 \rangle = 0.075$
- Doubly periodic
- 16 cm x 64 cm
- 0.25 cm grids

Model predictions

Bimodal PSD (e = 0.95)

Bidisperse Monodisperse ϕ

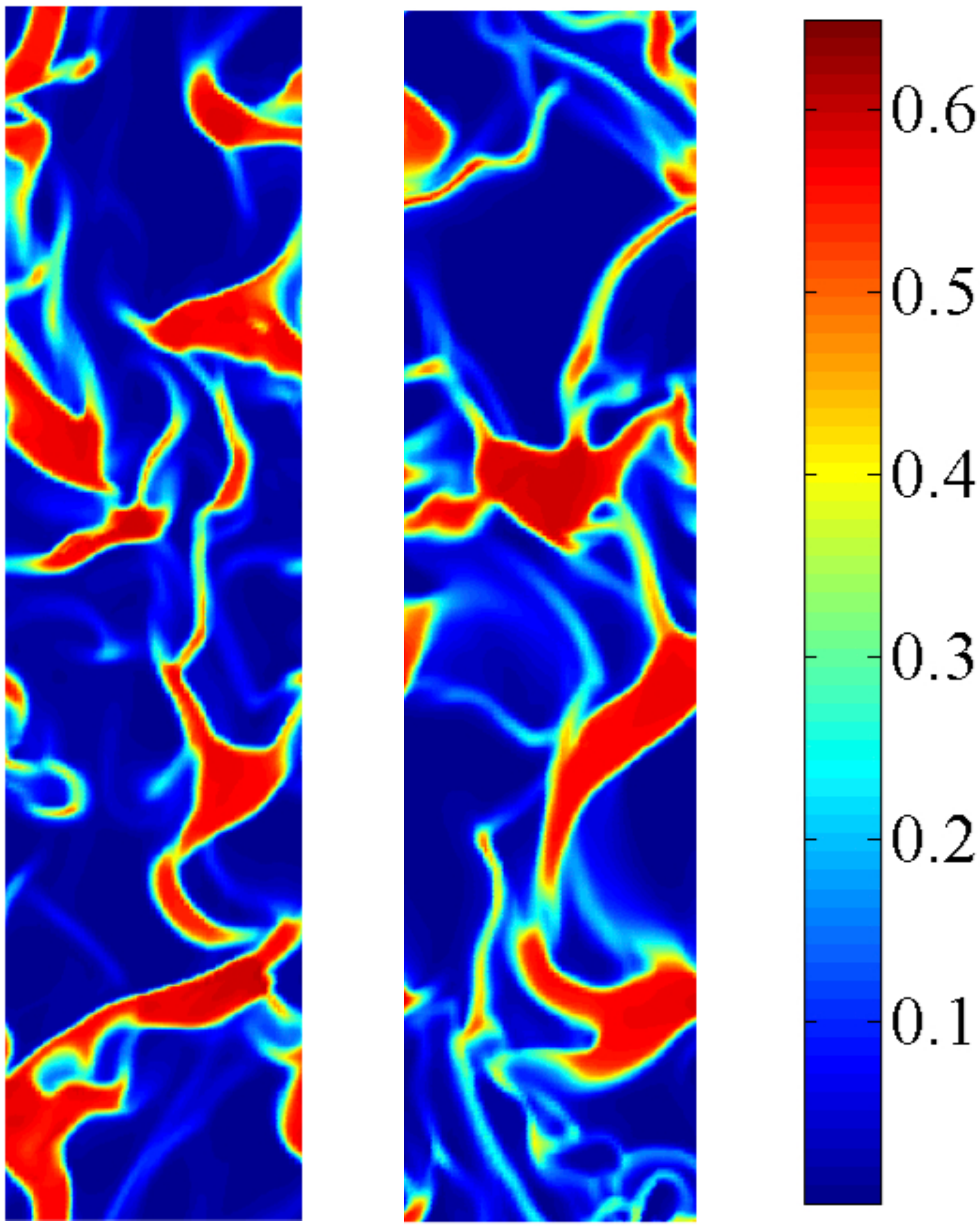

$$\langle V_{slip} \rangle = \frac{\langle (1-\phi) V_g \rangle}{\langle 1-\phi \rangle} - \frac{\langle \phi V_{s_{mix}} \rangle}{\langle \phi \rangle}$$

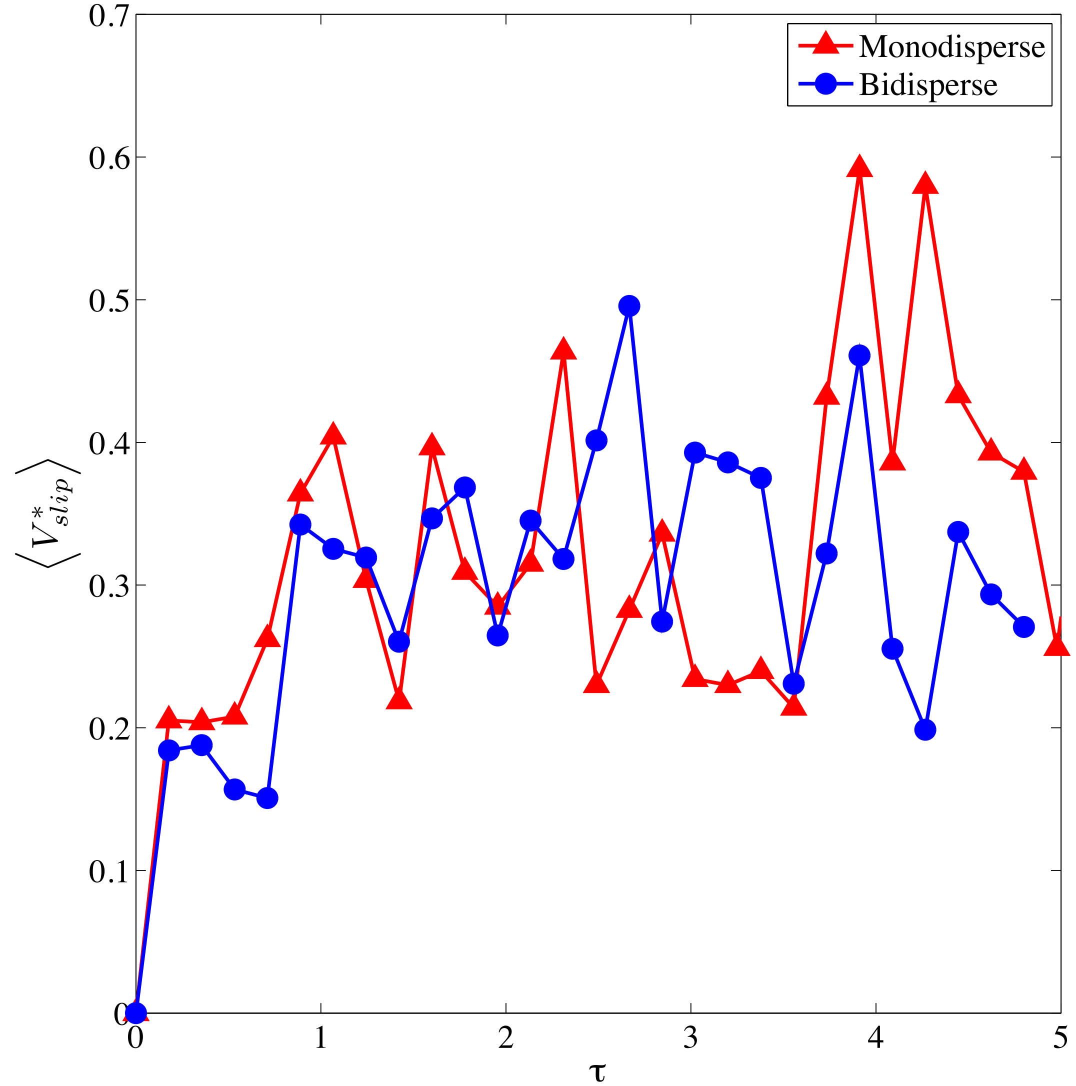

$$\langle V^*_{slip} \rangle = \frac{\langle V_{slip} \rangle}{V_t}$$

MFIX simulations:

- d_1=650 μm, d_2=170 μm
- $\langle \phi_1 \rangle = \langle \phi_2 \rangle = 0.075$
- Doubly periodic
- 16 cm x 64 cm
- 0.25 cm grids

$$\tau = t \frac{g}{V_t}$$

Model predictions

Bimodal PSD ($e = 0.99$)

Model predictions

Bimodal PSD (e = 0.99)

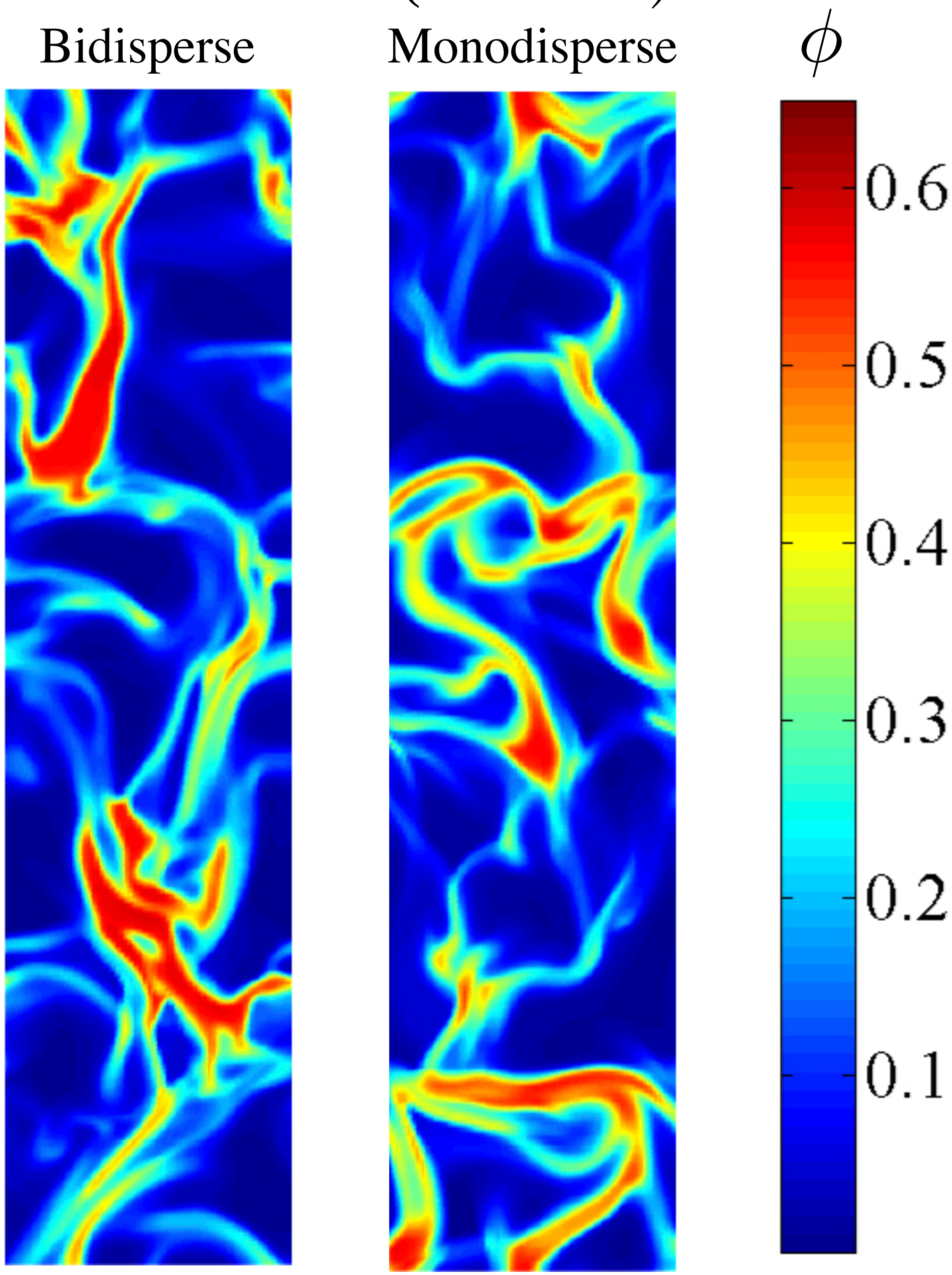

MFIX simulations:

- d_1=650 μm, d_2=170 μm
- $\langle \phi_1 \rangle = \langle \phi_2 \rangle = 0.075$
- Doubly periodic
- 16 cm x 64 cm
- 0.25 cm grids

Model predictions

Bimodal PSD (e = 0.99)

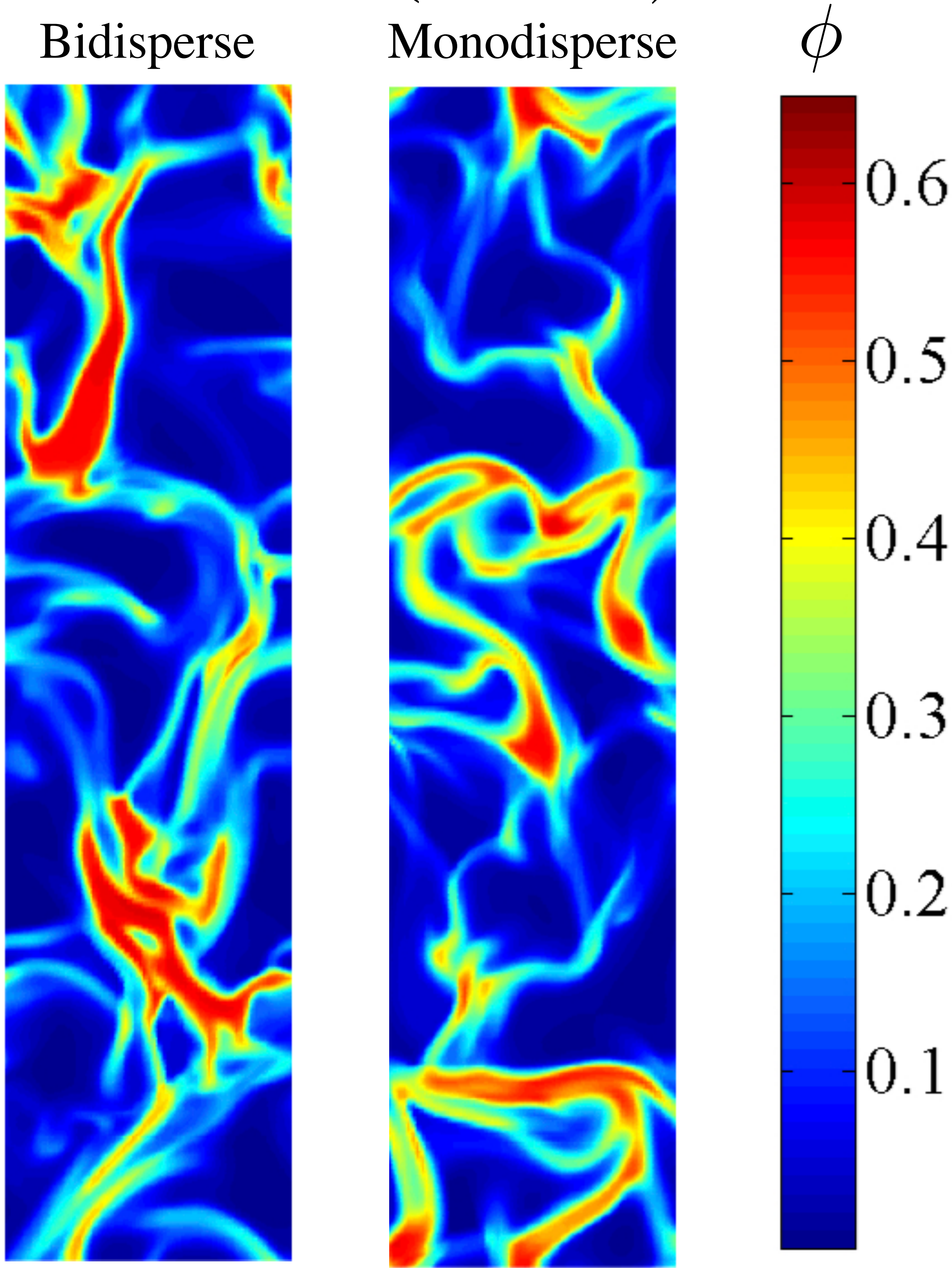

$$\langle V_{slip} \rangle = \frac{\langle (1-\phi) V_g \rangle}{\langle 1-\phi \rangle} - \frac{\langle \phi V_{s_{mix}} \rangle}{\langle \phi \rangle}$$

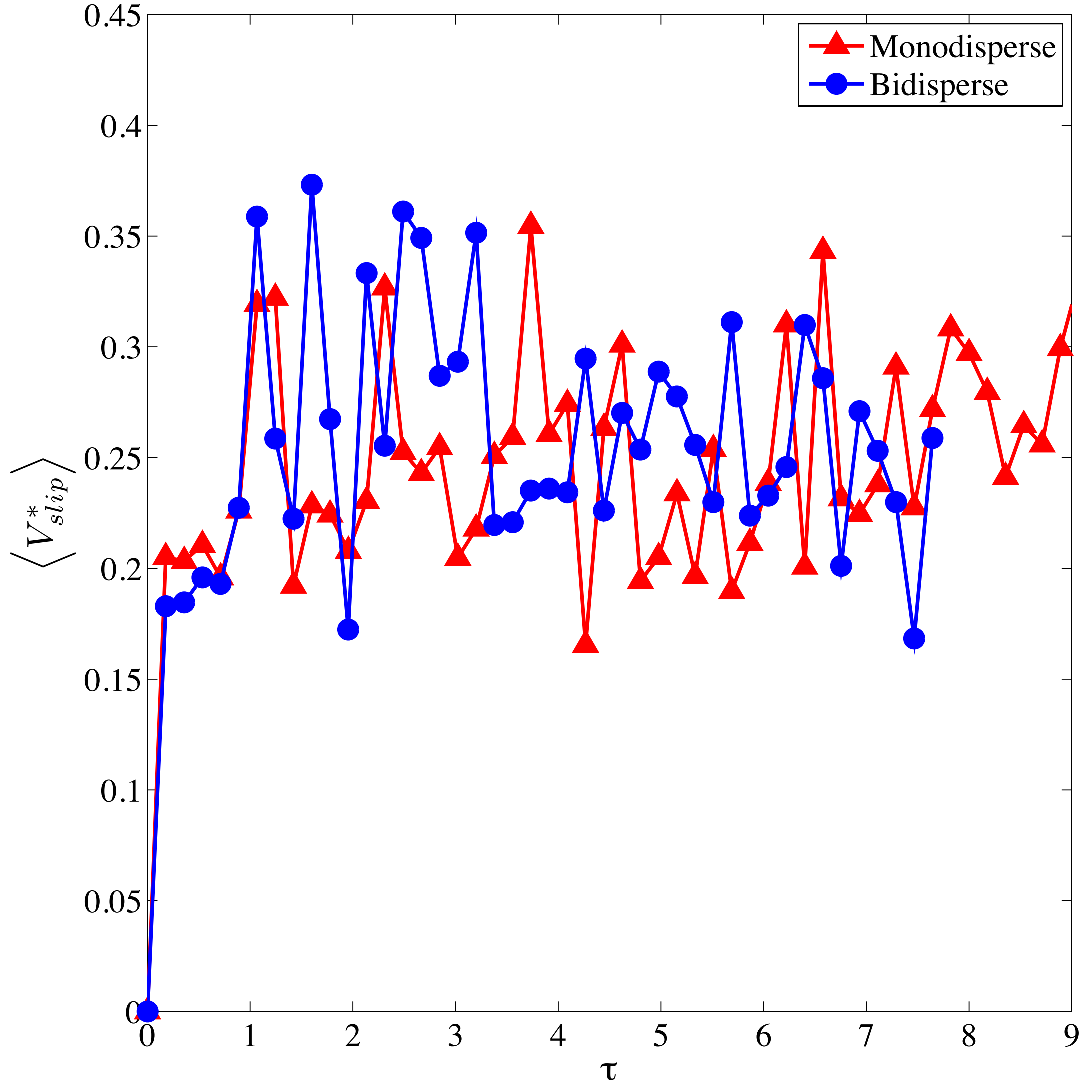

$$\langle V^*_{slip} \rangle = \frac{\langle V_{slip} \rangle}{V_t}$$

MFIX simulations:

- d_1=650 μm, d_2=170 μm
- $\langle \phi_1 \rangle = \langle \phi_2 \rangle = 0.075$
- Doubly periodic
- 16 cm x 64 cm
- 0.25 cm grids

$$\tau = t \frac{g}{V_t}$$

Model prediction: Volume fraction ratios

Bimodal PSD

Model prediction: Volume fraction ratios

Bimodal PSD

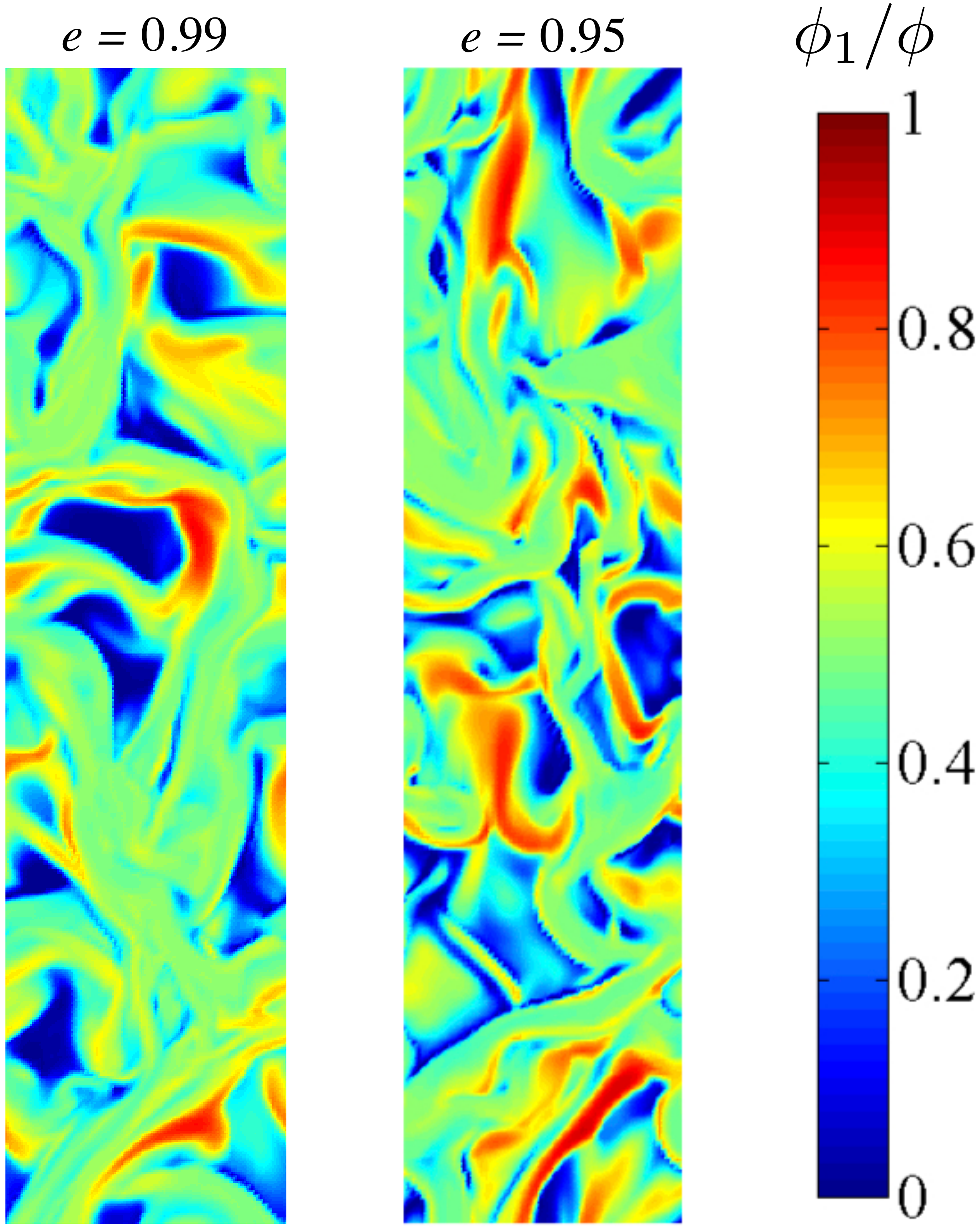

MFIX simulations:

- GHD theory
- HYS drag model
- d_1=650 μm, d_2=170 μm
- $\langle\phi_1\rangle$= 0.075, $\langle\phi_2\rangle$= 0.075
- Doubly periodic
- 16 cm x 64 cm

Model prediction: Volume fraction ratios

Bimodal PSD

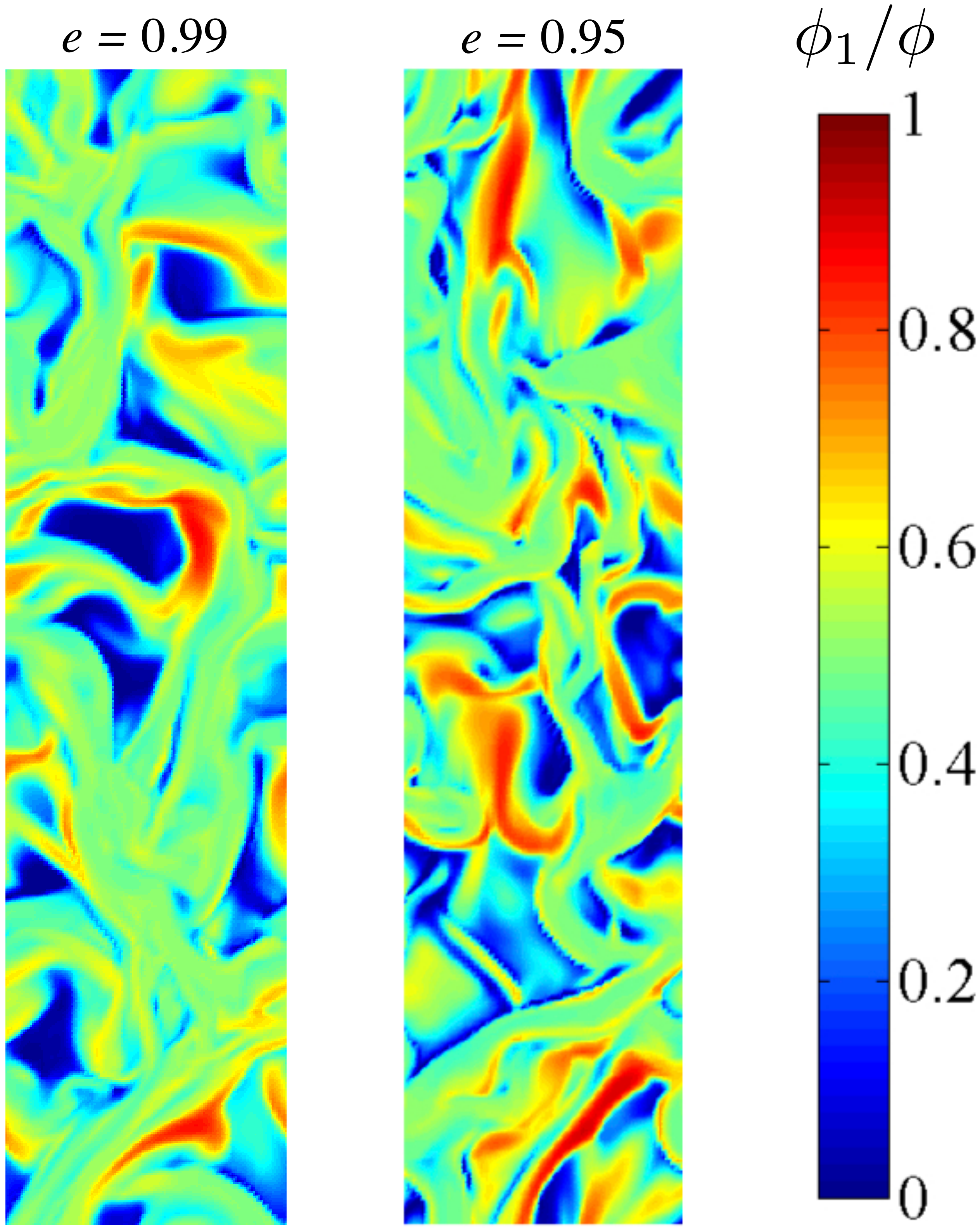

MFIX simulations:

- GHD theory
- HYS drag model
- d_1=650 μm, d_2=170 μm
- $\langle\phi_1\rangle$= 0.075, $\langle\phi_2\rangle$= 0.075
- Doubly periodic
- 16 cm x 64 cm

Bimodal PSD has a much broader distribution of particle volume fraction ratio than the Broad PSD case.

Grid resolution effects

Broad PSD ($e = 0.99$)

Grid resolution effects

Broad PSD (e = 0.99)

1 cm grids

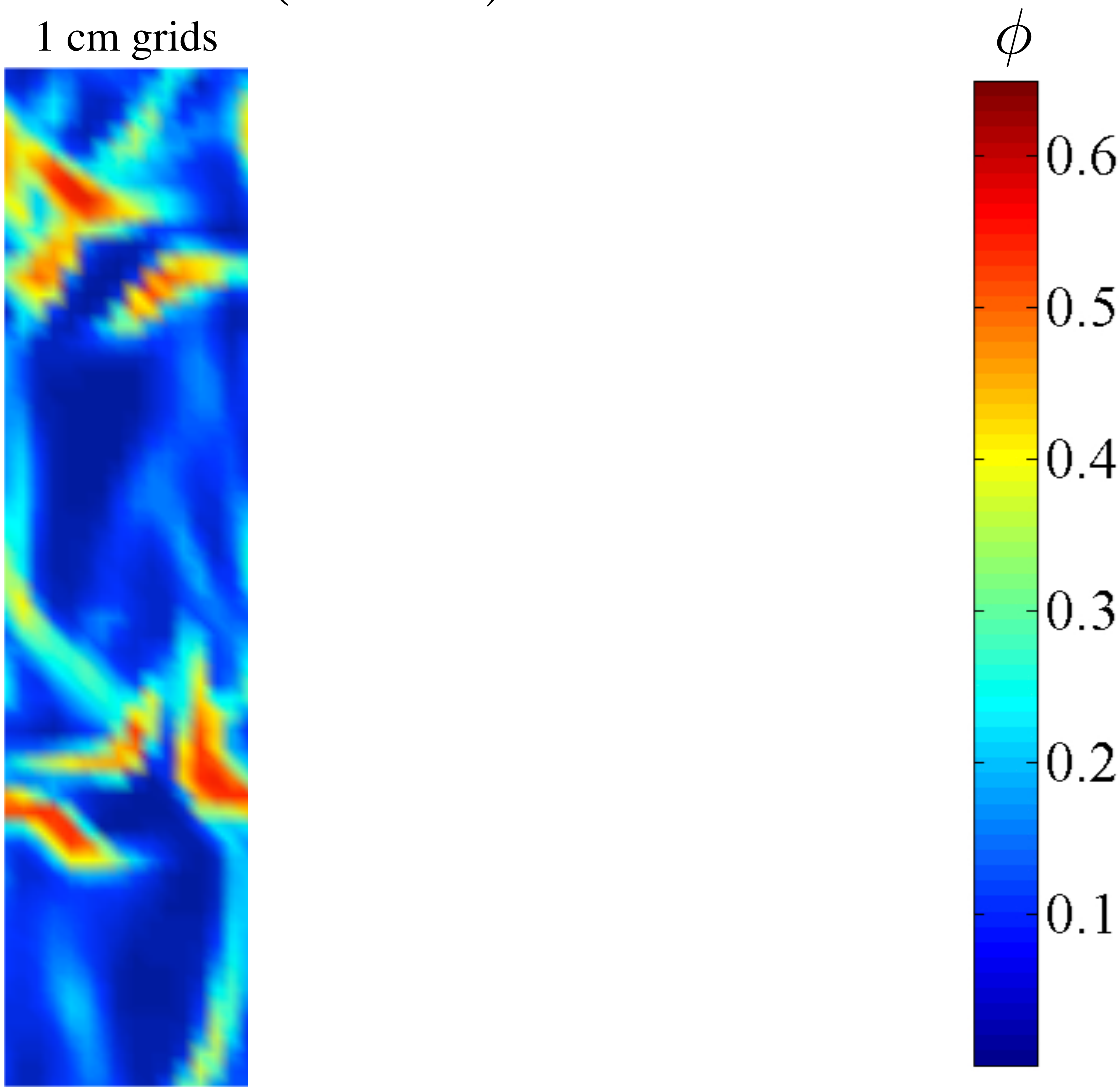

MFIX simulations:

- GHD theory
- HYS drag model
- d_1=212.5 μm, d_2=127.5 μm
- $\langle\phi_1\rangle$= 0.125, $\langle\phi_2\rangle$= 0.025
- Doubly periodic
- 16 cm x 64 cm

Grid resolution effects

Broad PSD (e = 0.99)

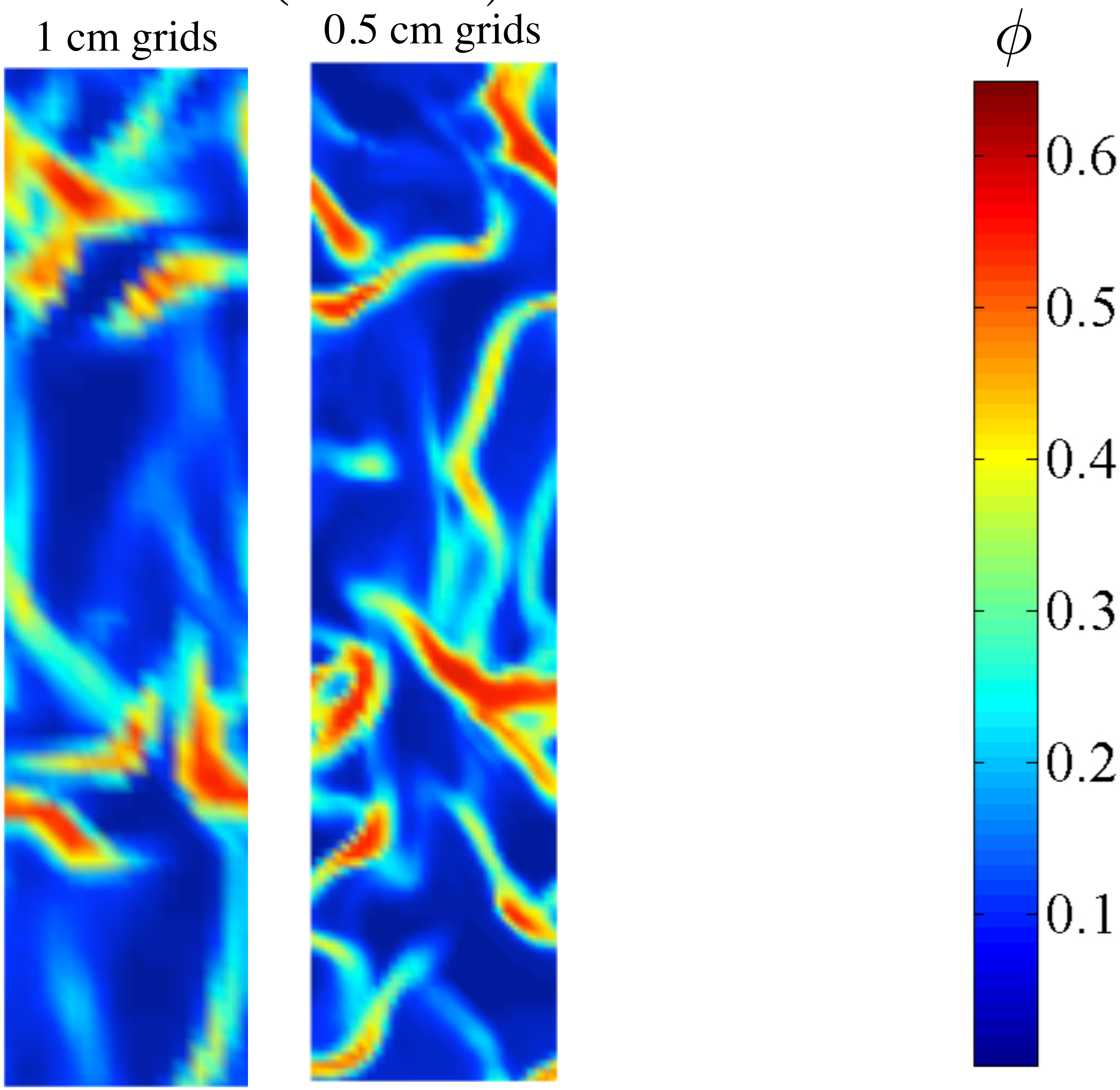

MFIX simulations:

- GHD theory
- HYS drag model
- d_1=212.5 μm, d_2=127.5 μm
- $\langle\phi_1\rangle$= 0.125, $\langle\phi_2\rangle$= 0.025
- Doubly periodic
- 16 cm x 64 cm

Grid resolution effects

Broad PSD (e = 0.99)

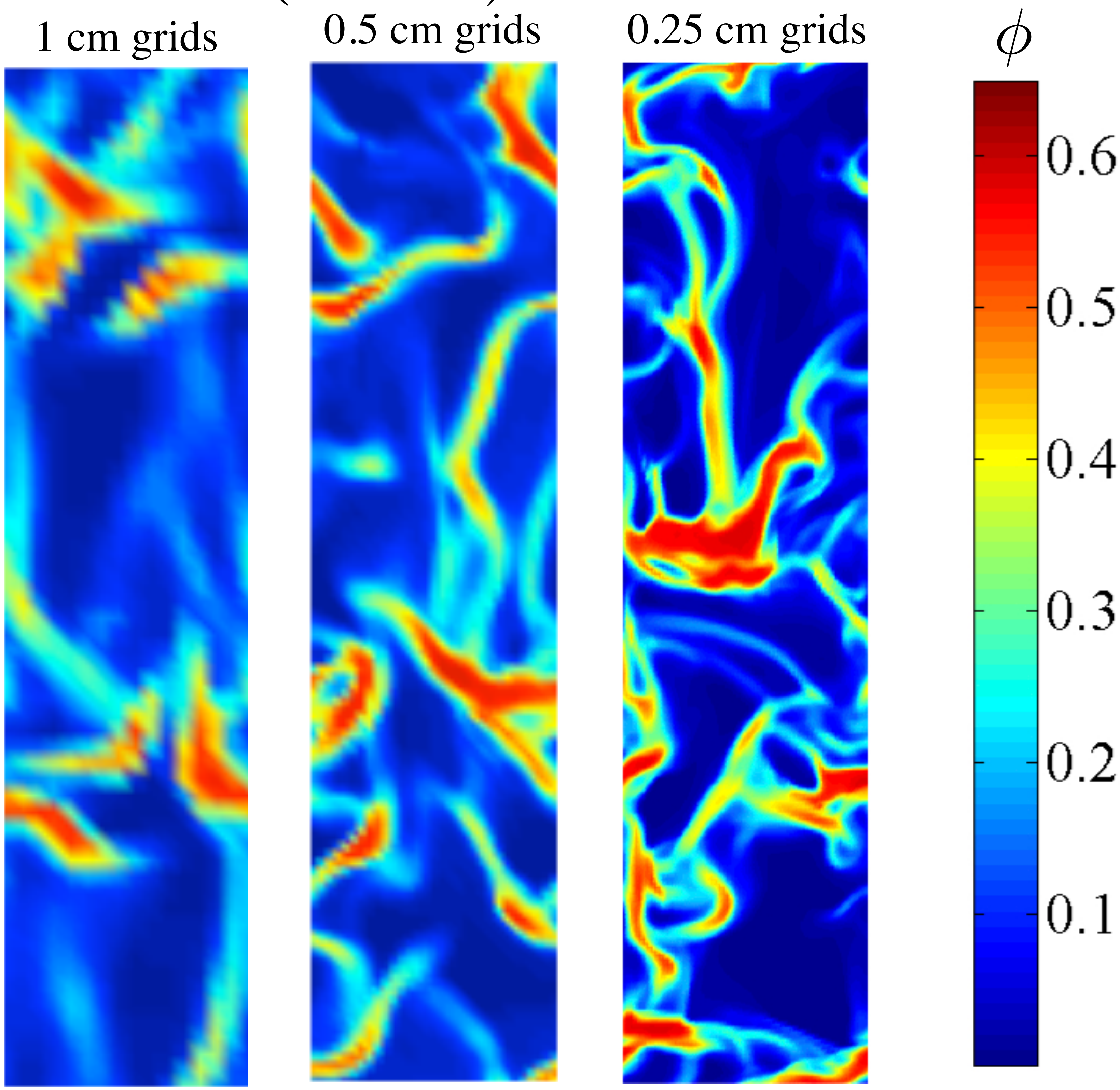

MFIX simulations:

- GHD theory
- HYS drag model
- d_1=212.5 μm, d_2=127.5 μm
- $\langle\phi_1\rangle$= 0.125, $\langle\phi_2\rangle$= 0.025
- Doubly periodic
- 16 cm x 64 cm

Grid resolution effects

Broad PSD (e = 0.99)

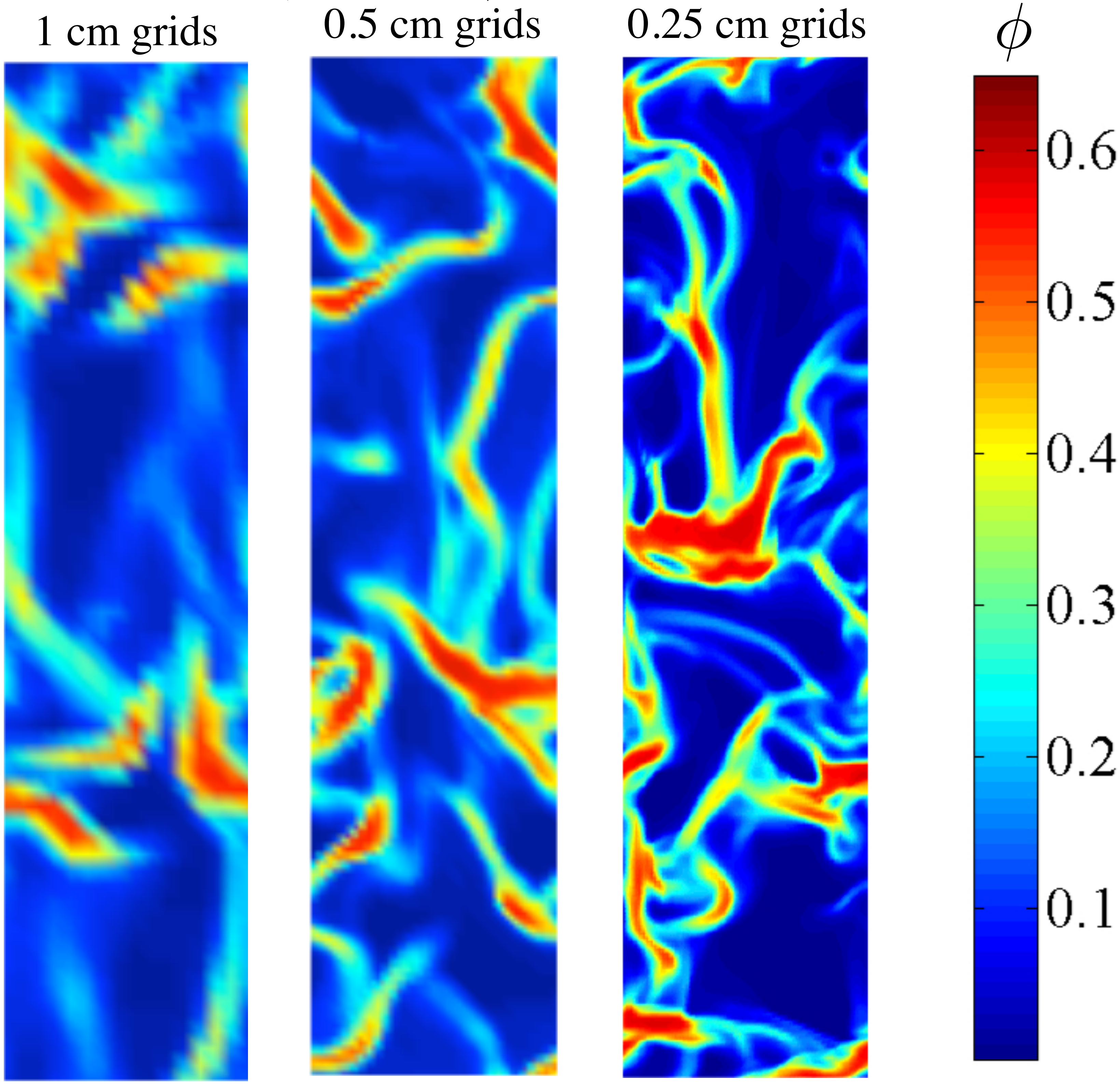

MFIX simulations:

- GHD theory
- HYS drag model
- d_1=212.5 μm, d_2=127.5 μm
- $\langle\phi_1\rangle$= 0.125, $\langle\phi_2\rangle$= 0.025
- Doubly periodic
- 16 cm x 64 cm

As grid resolution is increased, finer structures begin to appear in the flow domain.

Grid resolution effects

Bimodal PSD ($e = 0.99$**)**

Grid resolution effects

Bimodal PSD (e = 0.99)

1 cm grids

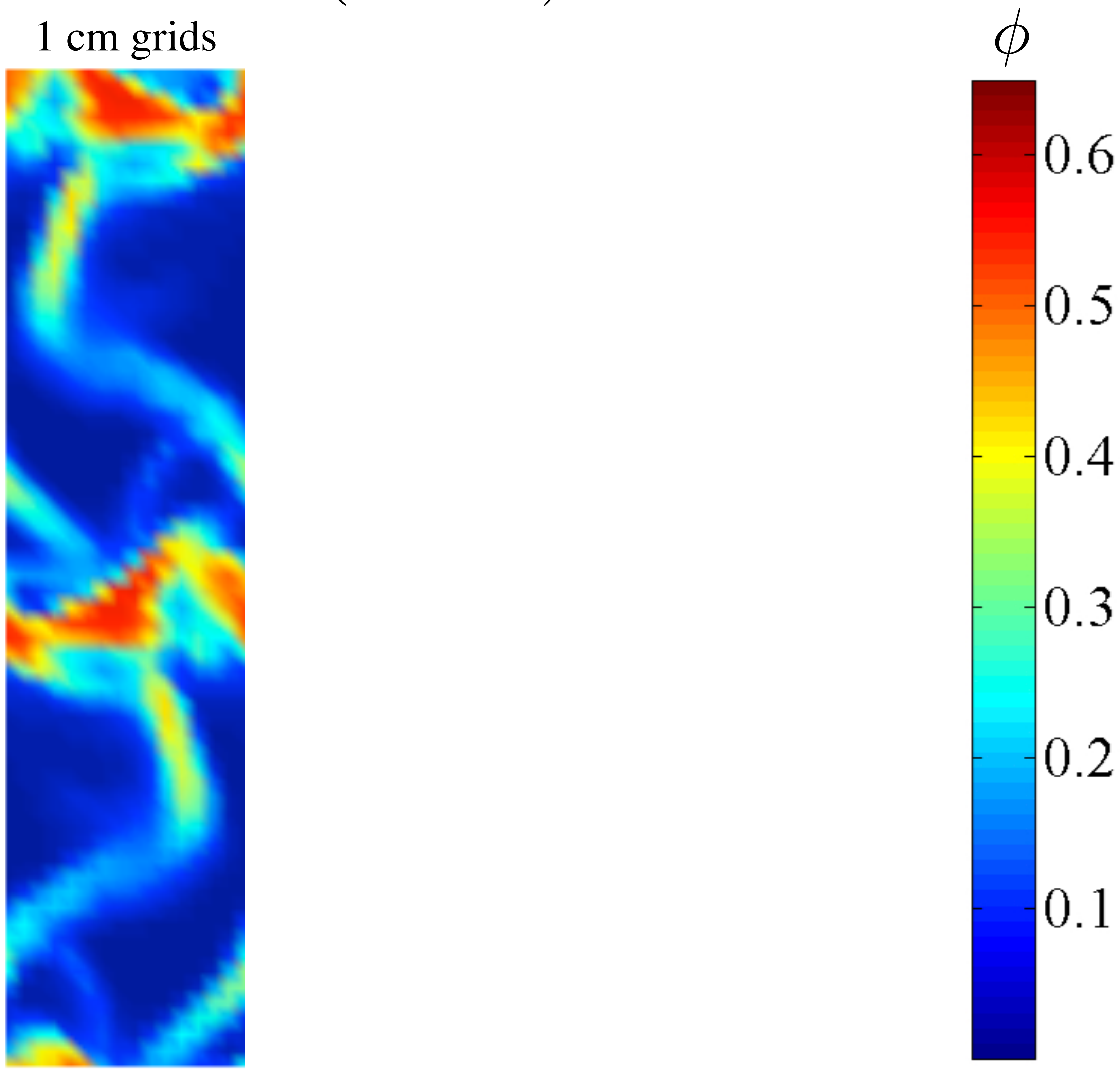

MFIX simulations:

- GHD theory
- HYS drag model
- d_1=650 μm, d_2=170 μm
- $\langle\phi_1\rangle$= 0.075, $\langle\phi_2\rangle$= 0.075
- Doubly periodic
- 16 cm x 64 cm

Grid resolution effects

Bimodal PSD (e = 0.99)

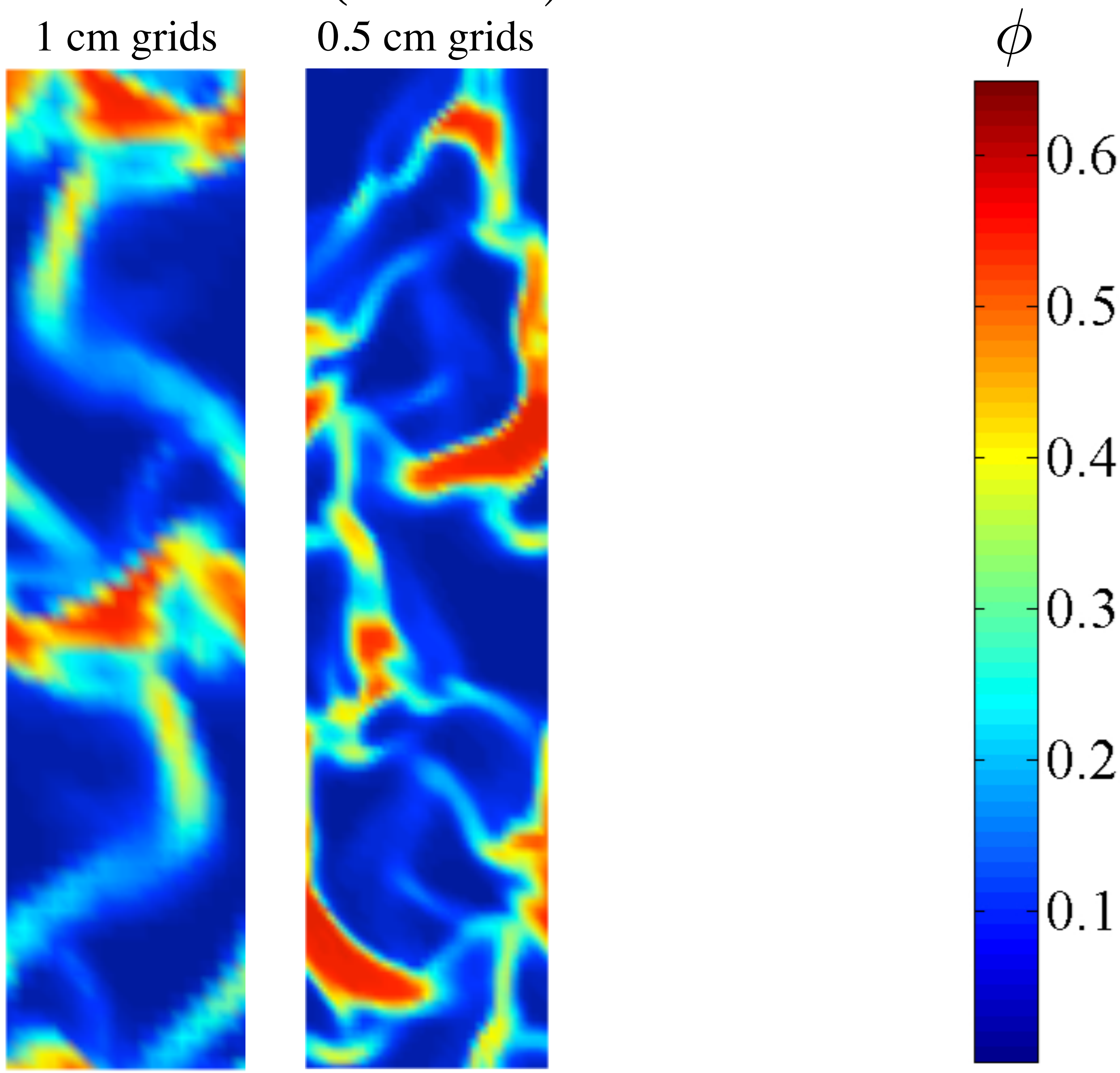

MFIX simulations:

- GHD theory
- HYS drag model
- d_1=650 μm, d_2=170 μm
- $\langle\phi_1\rangle$= 0.075, $\langle\phi_2\rangle$= 0.075
- Doubly periodic
- 16 cm x 64 cm

Grid resolution effects

Bimodal PSD (e = 0.99)

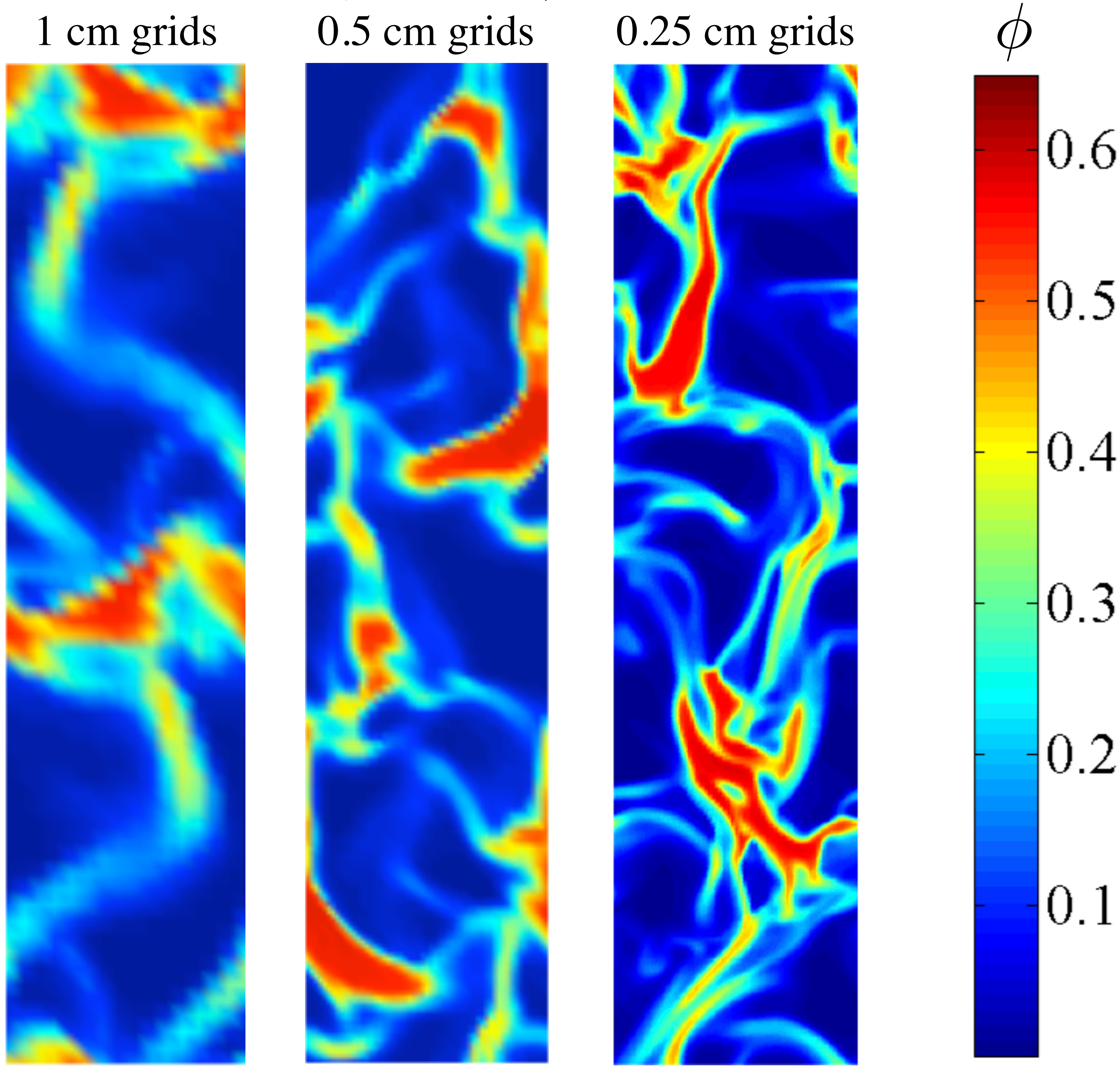

MFIX simulations:

- GHD theory
- HYS drag model
- d_1=650 μm, d_2=170 μm
- $\langle\phi_1\rangle$= 0.075, $\langle\phi_2\rangle$= 0.075
- Doubly periodic
- 16 cm x 64 cm

Grid resolution effects

Bimodal PSD (e = 0.99)

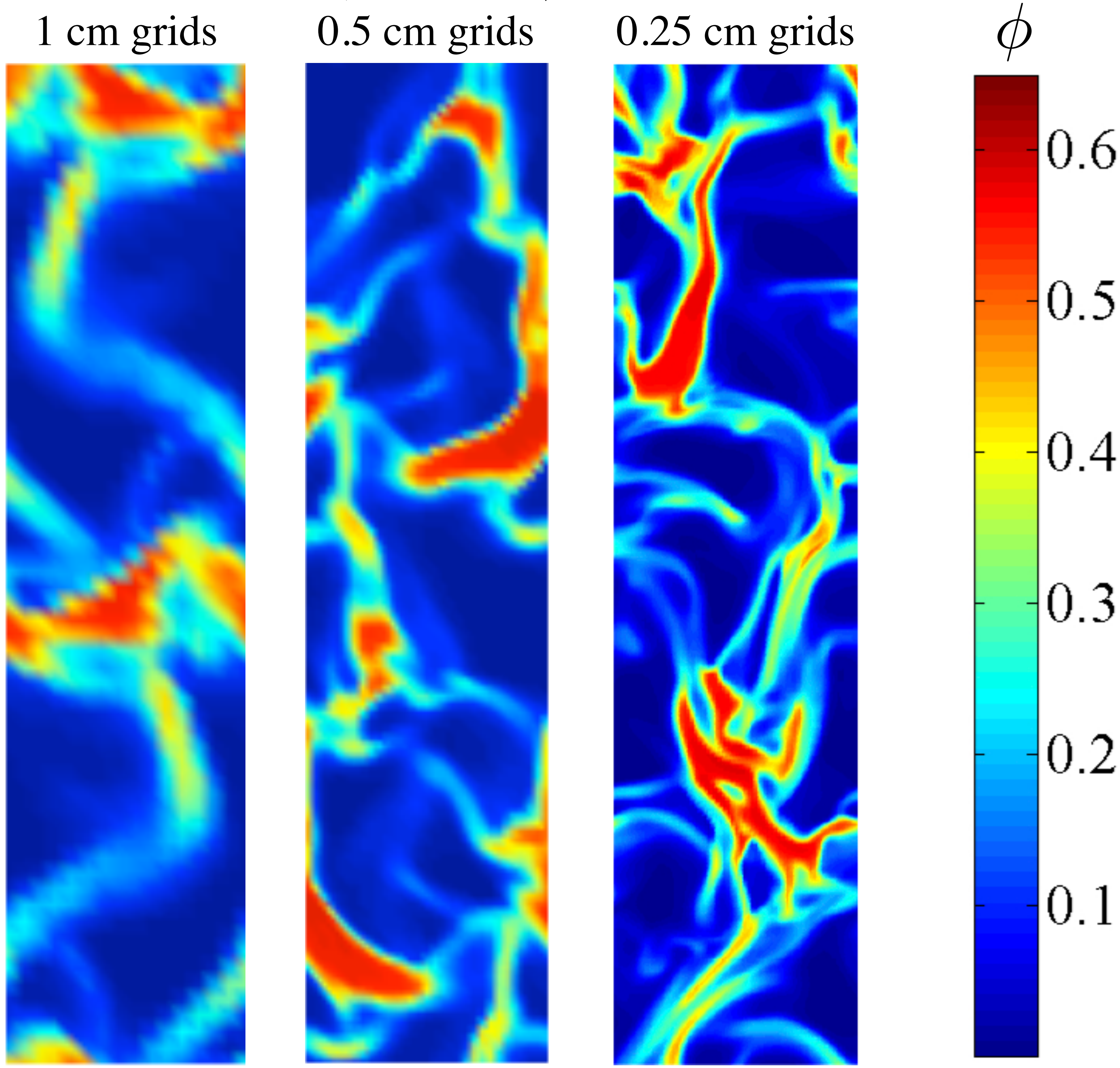

MFIX simulations:

- GHD theory
- HYS drag model
- d_1=650 μm, d_2=170 μm
- $\langle\phi_1\rangle$= 0.075, $\langle\phi_2\rangle$= 0.075
- Doubly periodic
- 16 cm x 64 cm

The emergence of fine structure with grid resolution indicates that equations used to model binary gas-solid flows must be coarse grained.

Range of validity of kinetic theory formulation

Bimodal PSD ($e = 0.95$)

Assumption:
$Kn << 1$

$$Kn = \frac{l_{mf}}{l_{grad}}$$

$$l_{mf} \approx \frac{d}{6\sqrt{2}\phi}$$

$$l_{grad} = \left| \frac{\bar{\chi}}{\nabla \chi} \right|$$

Range of validity of kinetic theory formulation

Bimodal PSD ($e = 0.95$)

$$\boxed{\text{Assumption: } Kn << 1}$$

$$Kn = \frac{l_{mf}}{l_{grad}}$$

$$l_{mf} \approx \frac{d}{6\sqrt{2}\phi}$$

$$l_{grad} = \left| \frac{\bar{\chi}}{\nabla \chi} \right|$$

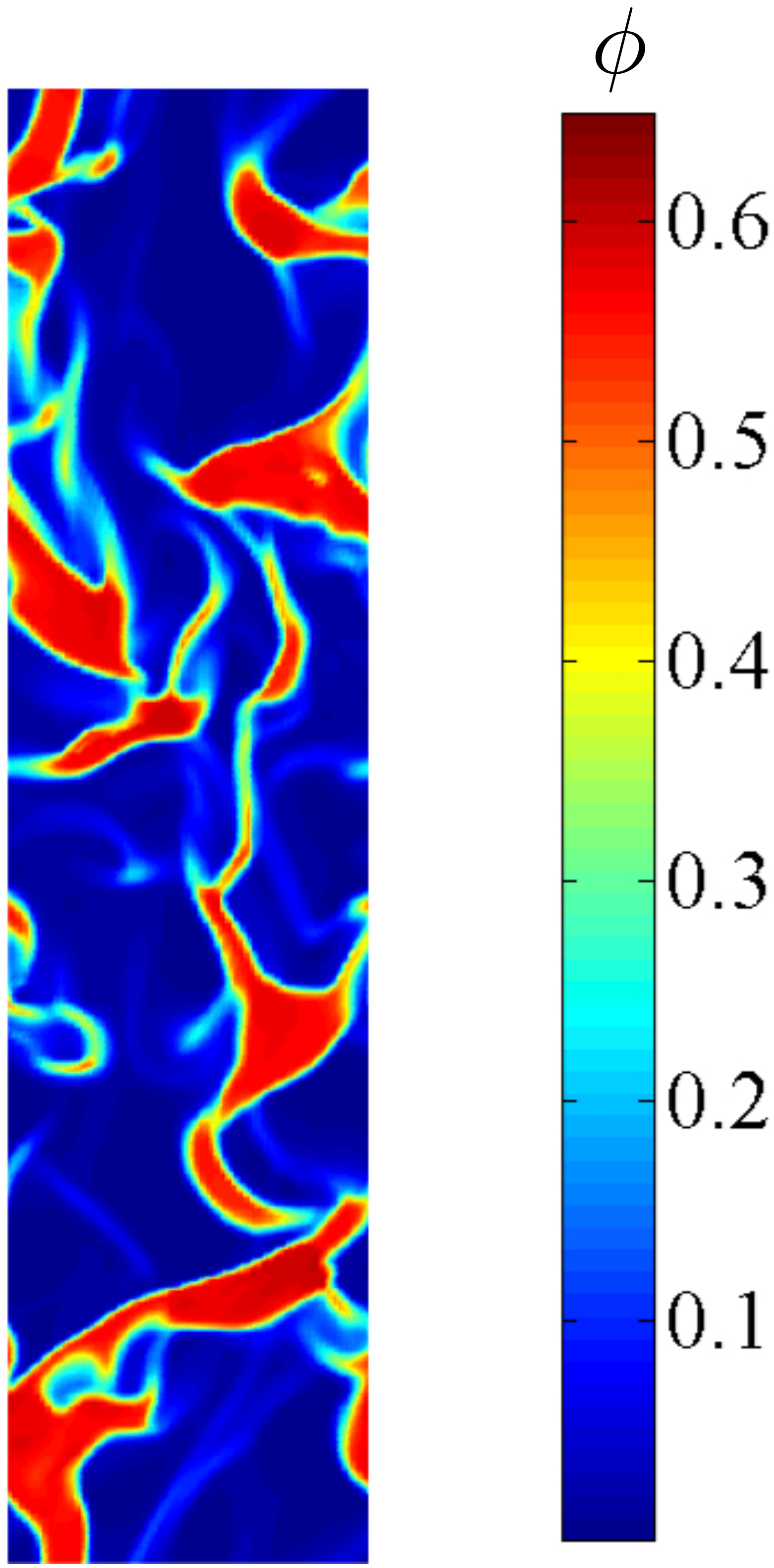

Range of validity of kinetic theory formulation

Bimodal PSD ($e = 0.95$)

Assumption:
$Kn << 1$

$$Kn = \frac{l_{mf}}{l_{grad}}$$

$$l_{mf} \approx \frac{d}{6\sqrt{2}\phi}$$

$$l_{grad} = \left| \frac{\bar{\chi}}{\nabla \chi} \right|$$

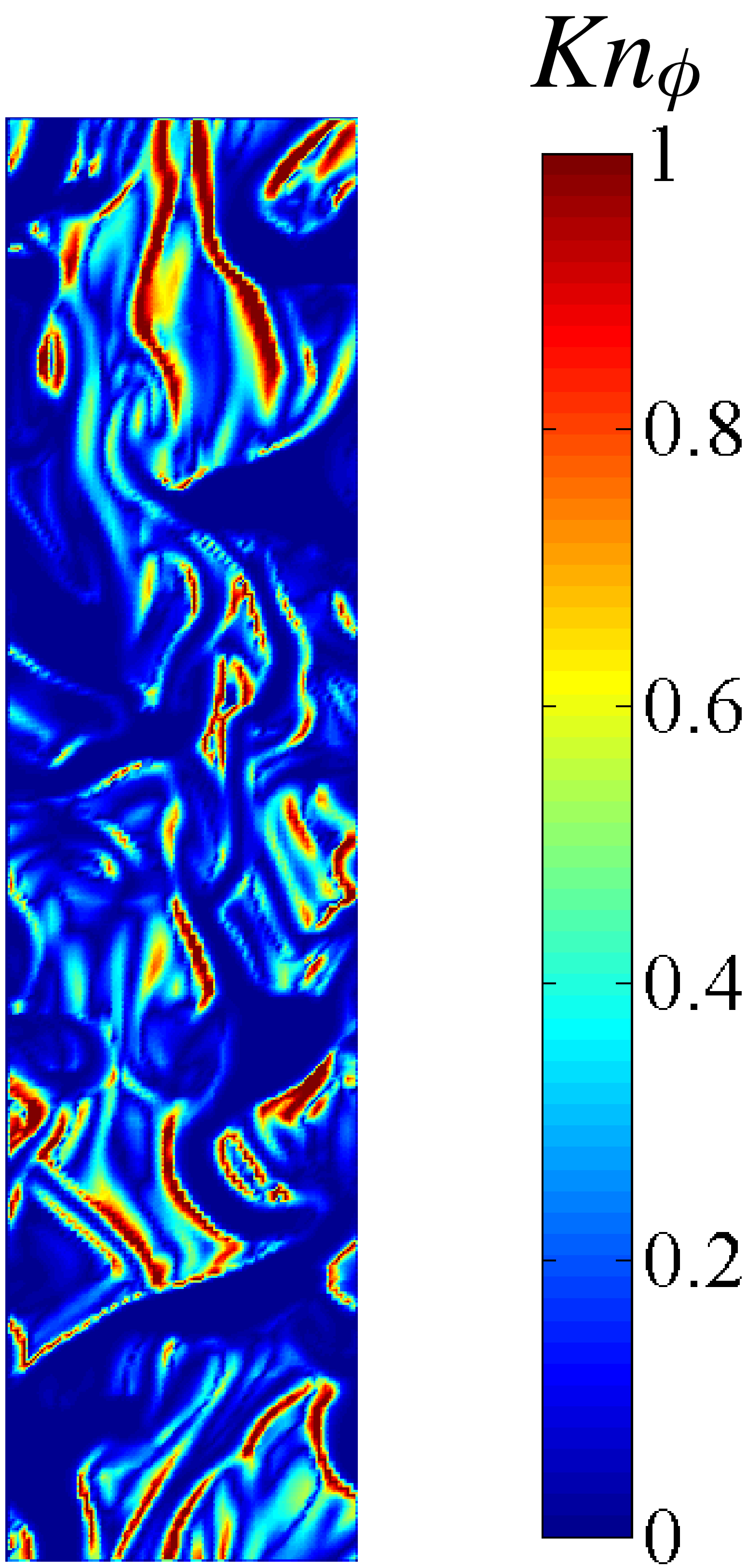

Range of validity of kinetic theory formulation

Bimodal PSD ($e = 0.95$)

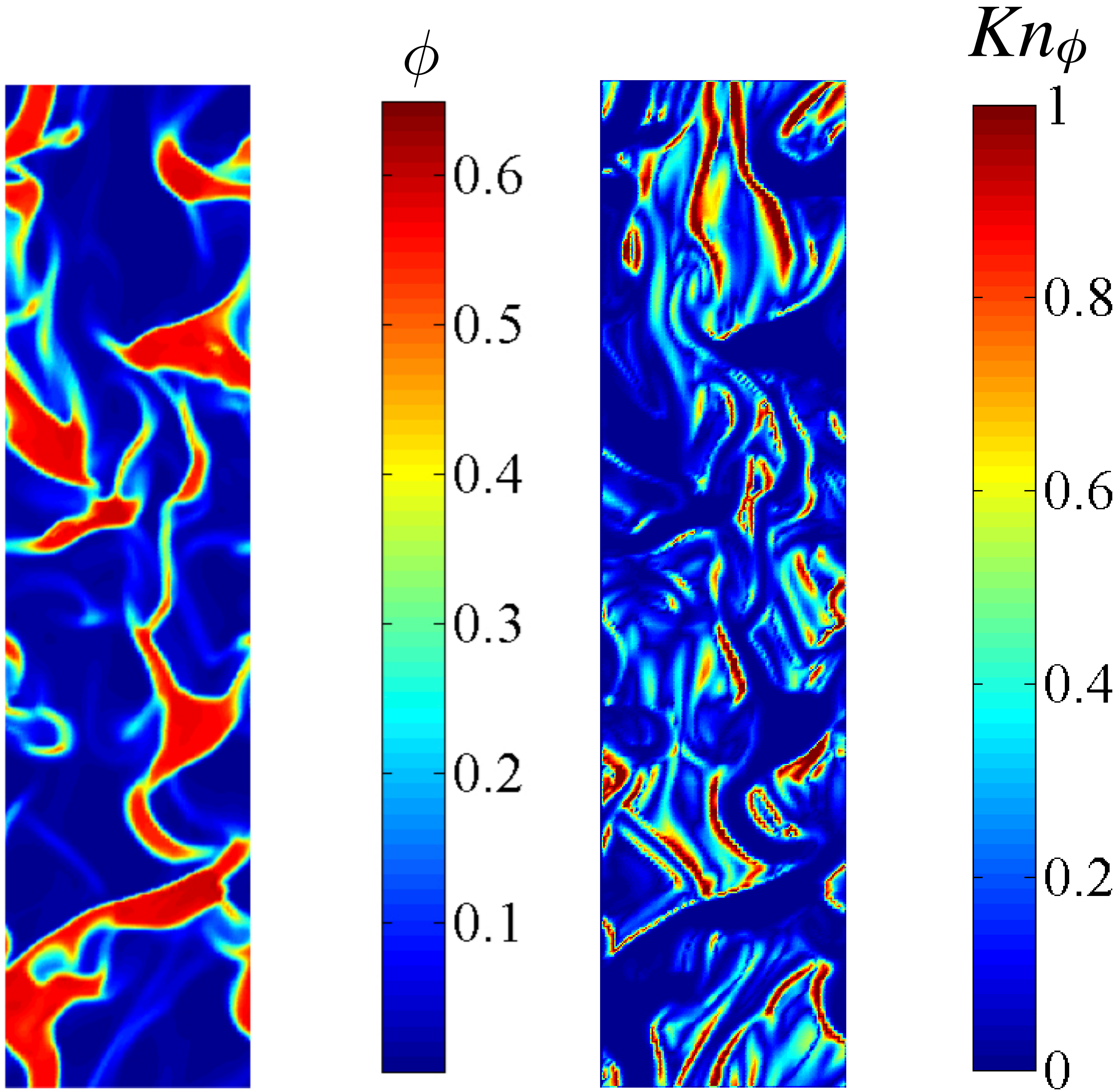

Assumption:
$Kn << 1$

$$Kn = \frac{l_{mf}}{l_{grad}}$$

$$l_{mf} \approx \frac{d}{6\sqrt{2}\phi}$$

$$l_{grad} = \left| \frac{\bar{\chi}}{\nabla \chi} \right|$$

Range of validity of kinetic theory formulation

Bimodal PSD ($e = 0.95$)

$$\boxed{\begin{array}{c}\text{Assumption:}\\ Kn << 1\end{array}}$$

$$Kn = \frac{l_{mf}}{l_{grad}}$$

$$l_{mf} \approx \frac{d}{6\sqrt{2}\phi}$$

$$l_{grad} = \left| \frac{\bar{\chi}}{\nabla \chi} \right|$$

Range of validity of kinetic theory formulation

Bimodal PSD (e = 0.95)

Assumption:
$Kn << 1$

$$Kn = \frac{l_{mf}}{l_{grad}}$$

$$l_{mf} \approx \frac{d}{6\sqrt{2}\phi}$$

$$l_{grad} = \left|\frac{\bar{\chi}}{\nabla \chi}\right|$$

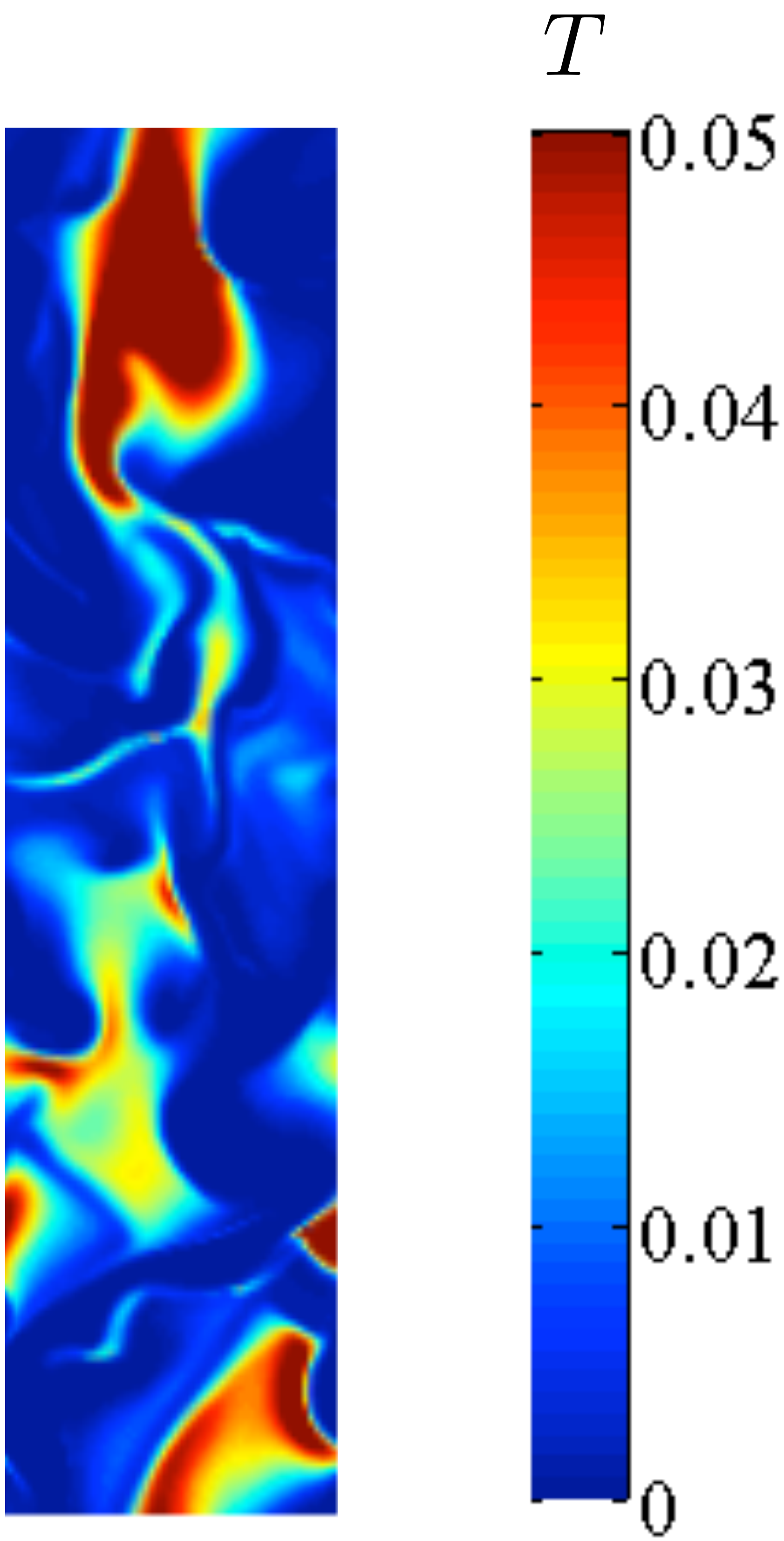

Range of validity of kinetic theory formulation

Bimodal PSD (e = 0.95)

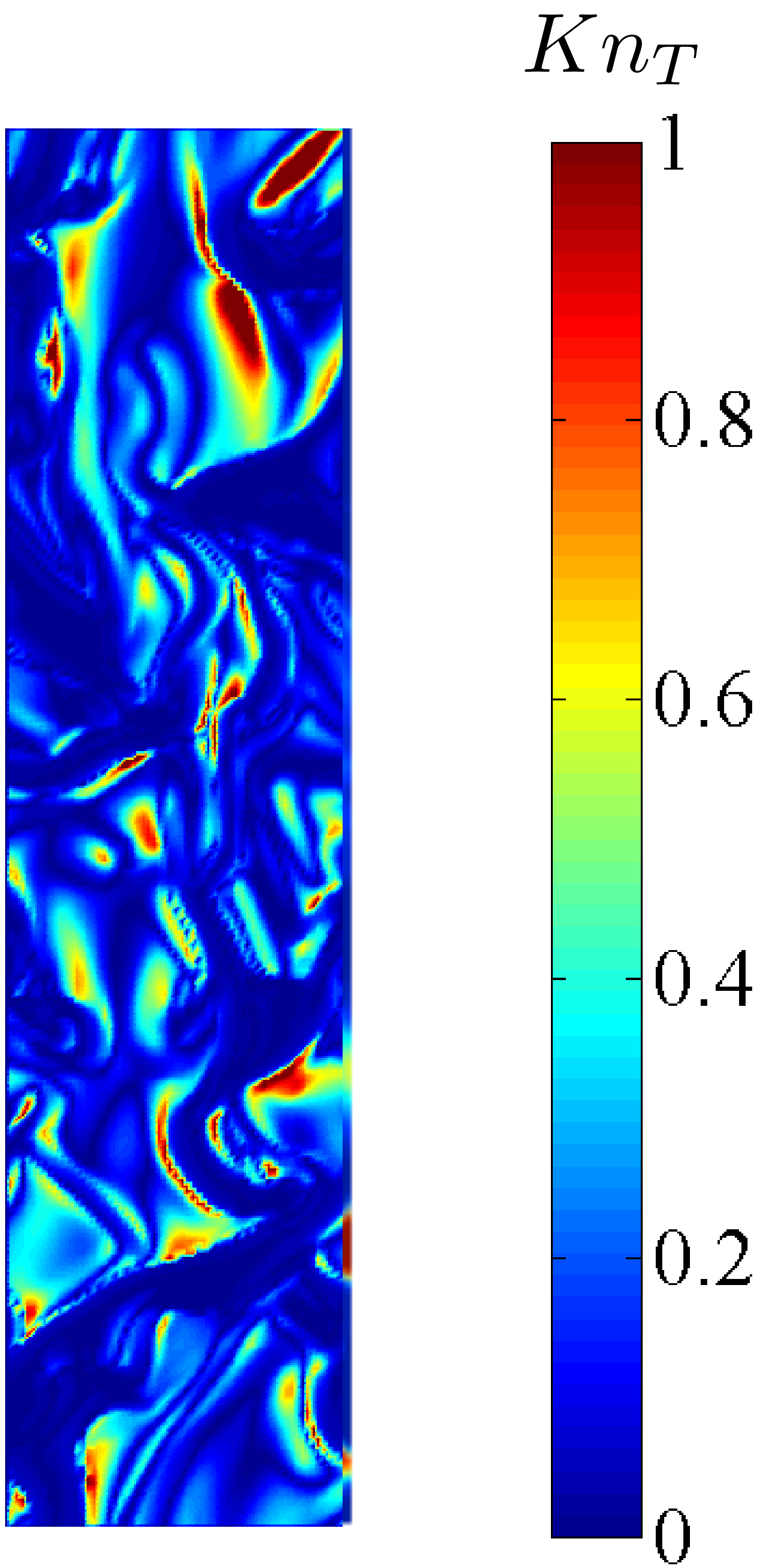

Assumption:
$Kn << 1$

$$Kn = \frac{l_{mf}}{l_{grad}}$$

$$l_{mf} \approx \frac{d}{6\sqrt{2}\phi}$$

$$l_{grad} = \left| \frac{\bar{\chi}}{\nabla \chi} \right|$$

Range of validity of kinetic theory formulation

Bimodal PSD (e = 0.95)

Assumption:
$Kn << 1$

$$Kn = \frac{l_{mf}}{l_{grad}}$$

$$l_{mf} \approx \frac{d}{6\sqrt{2}\phi}$$

$$l_{grad} = \left| \frac{\bar{\chi}}{\nabla \chi} \right|$$

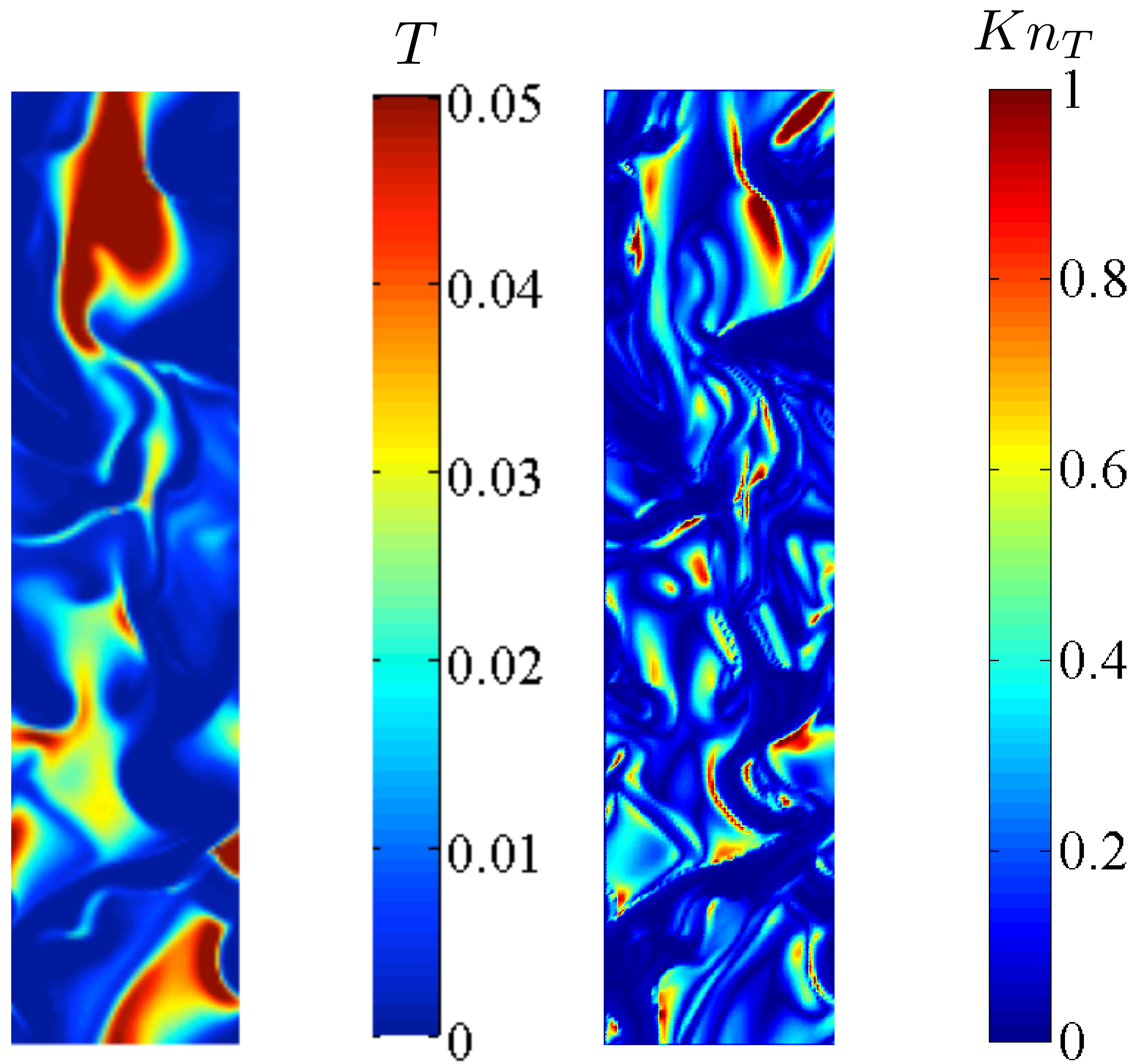

Summary

Summary

- HYS drag model has been implemented within new CVS version of MFIX.

Summary

- HYS drag model has been implemented within new CVS version of MFIX.
- GHD theory has been implemented within MFIX and operates robustly, even in very inhomogeneous gas-solid flows.

Summary

- HYS drag model has been implemented within new CVS version of MFIX.
- GHD theory has been implemented within MFIX and operates robustly, even in very inhomogeneous gas-solid flows.
- Binary fluidized gas-solid suspensions manifest inhomogeneous structures similar to monodisperse systems.

Summary

- HYS drag model has been implemented within new CVS version of MFIX.
- GHD theory has been implemented within MFIX and operates robustly, even in very inhomogeneous gas-solid flows.
- Binary fluidized gas-solid suspensions manifest inhomogeneous structures similar to monodisperse systems.
- Volume averaged slip velocities in both monodisperse and bidisperse gas-solid flows are qualitatively similar when both PSDs have the same Sauter mean diameter.

Summary

- HYS drag model has been implemented within new CVS version of MFIX.
- GHD theory has been implemented within MFIX and operates robustly, even in very inhomogeneous gas-solid flows.
- Binary fluidized gas-solid suspensions manifest inhomogeneous structures similar to monodisperse systems.
- Volume averaged slip velocities in both monodisperse and bidisperse gas-solid flows are qualitatively similar when both PSDs have the same Sauter mean diameter.
- The scale of structures in binary gas-solid flows depends on grid resolution, similar to monodisperse suspensions.

Summary

- HYS drag model has been implemented within new CVS version of MFIX.
- GHD theory has been implemented within MFIX and operates robustly, even in very inhomogeneous gas-solid flows.
- Binary fluidized gas-solid suspensions manifest inhomogeneous structures similar to monodisperse systems.
- Volume averaged slip velocities in both monodisperse and bidisperse gas-solid flows are qualitatively similar when both PSDs have the same Sauter mean diameter.
- The scale of structures in binary gas-solid flows depends on grid resolution, similar to monodisperse suspensions.
- Knudsen number was found to be $O(1)$ or less throughout simulation domain.

Acknowledgements

People:
- Jin Sun
- Sebastian Chialvo
- Yesim Igci
- Jia Chew

Funding:
- US Department of Energy
- ExxonMobil Corporation
- ACS Petroleum Research Fund